Atmos. Chem. Phys. Discuss., doi:10.5194/acp-2016-438, 2016
Manuscript under review for journal Atmos. Chem. Phys.
Published: 2 June 2016


Atmospheric Chemistry and Physics Discussions

# Heterogeneous ice nucleation on dust particles sourced from 9 deserts worldwide - Part 1: Immersion freezing

Yvonne Boose[1], André Welti[1,2], James Atkinson[1], Fabiola Ramelli[1], Anja Danielczok[3], Heinz G. Bingemer[3], Michael Plötze[4], Berko Sierau[1], Zamin A. Kanji[1], and Ulrike Lohmann[1]

[1]Institute for Atmospheric and Climate Science, ETH Zürich, Zürich, Switzerland
[2]now at Leibniz Institute for Tropospheric Research, Leipzig, Germany
[3]Institute for Atmospheric and Environmental Sciences, J. W. Goethe-University, Frankfurt am Main, Germany
[4]Institute for Geotechnical Engineering, ETH Zürich, Zürich, Switzerland

*Correspondence to:* Y.Boose (yvonne.boose@env.ethz.ch) and Z. A. Kanji (zamin.kanji@env.ethz.ch)

**Abstract.** Desert dust is one of the most abundant ice nucleating particle types in the atmosphere. Traditionally, clay minerals were assumed to determine the ice nucleation ability of desert dust and constituted the focus of ice nucleation studies. Only recently some feldspar species were identified to be ice-active at much higher temperatures than clay minerals, redirecting studies to investigate the contribution of feldspar to ice nucleation on desert dust. However, so far no study has shown the atmospheric relevance of this mineral phase.

For this study four dust samples were collected after airborne transport in the troposphere from the Sahara to different locations (Crete, the Peloponnese, Canary Islands and the Sinai Peninsula). Additionally, eleven dust samples were collected from the surface from nine of the biggest deserts worldwide. The samples were used to study the ice nucleation behavior specific to different desert dusts. Furthermore we investigated how representative ice nucleation on surface-collected dust is for that in the atmosphere by comparing to the ice nucleation activity of the airborne samples. We used the IMCA-ZINC set-up to form droplets on single aerosol particles which were subsequently exposed to temperatures between 233 - 250 K. Dust particles were collected in parallel on filters for offline cold stage ice nucleation experiments at 253 - 263 K. To help the interpretation of the results from the ice nucleation experiments the mineralogical composition of the dusts was investigated. We found that a higher ice nucleation activity in a given sample can be attributed at 253 K to the K-feldspar content present in this sample whereas at temperatures between 238 - 245 K it is attributed to the sum of feldspar and quartz content present. A high clay content on the other hand is associated with a lower ice nucleation activity of a sample. This confirms the importance of feldspar at $T > 250$ K and the role of quartz and feldspars determining the ice nucleation activities at lower T as found by earlier studies for monomineral dust surrogates. Furthermore, we find that milling may lead to a decrease in the ice nucleation ability of polymineral samples due to a change in mineralogical composition in the atmospherically relevant size fraction arising from the different hardness and cleavage of individual mineral phases. Comparison of our comprehensive data set to an existing desert dust parameterization confirms its applicability for climate models. Our results suggest that for an improved prediction of the ice nucleation ability of desert dust in the atmosphere, the modelling of emission and atmospheric transport of the feldspar and quartz mineral phases would be key while other minerals are only of minor importance.

Atmos. Chem. Phys. Discuss., doi:10.5194/acp-2016-438, 2016
Manuscript under review for journal Atmos. Chem. Phys.
Published: 2 June 2016


Atmospheric Chemistry and Physics Discussions

## 1 Introduction

Predicting the occurrence and evolution of clouds at temperatures ($T$) below 273 K remains a challenge for global and regional climate models (Boucher et al., 2013). One source of uncertainty is the effect of certain aerosol particles which determine the cold cloud microphysics by acting as ice nucleating particles (INPs). Ice formation affects precipitation, cloud life time and radiative properties of these clouds and by that global climate (Lohmann and Feichter, 2005). Mineral dust particles have been known as efficient INPs at $T \leq 253$ K for more than 60 years (e.g. Isono 1955, and references given in Hoose and Möhler 2012; Murray et al. 2012) and have been observed to nucleate ice in the atmosphere in various regions worldwide (Kumai, 1976; DeMott et al., 2003; Chou et al., 2011; Boose et al., 2016a, b). However, the molecular mechanisms and particle properties triggering ice nucleation (IN) on atmospheric mineral dusts are still subject of ongoing research. Supercooled cloud droplets can freeze homogeneously at temperatures below 235 K, i.e. without the aid of an INP (Schaefer, 1946; Mason and Ludlam, 1950). At higher temperatures the surface of an INP is required to overcome the energy barrier of freezing. Traditionally, four pathways of ice nucleation are differentiated (Vali et al., 2015):

1) deposition nucleation where ice forms on an INP directly from the vapor phase;

2) condensation freezing which describes the process of ice forming during the process of water condensing on an INP;

3) immersion freezing where an INP immersed in a supercooled cloud droplet initiates freezing;

4) contact freezing where the interaction of an INP with the surface of a supercooled droplet either from the outside or inside of the droplet leads to freezing.

Ice formation in clouds with top temperatures above 263 K is often observed (Hobbs and Rangno, 1985) but only very few aerosol particle types have been identified to weakly nucleate ice at these warm temperatures. These are mainly biological particles, such as certain bacterial strains or macromolecules (Schnell and Vali, 1976; Krog et al., 1979; Möhler et al., 2008). The IN ability of soot (Brooks et al., 2014; Kulkarni et al., 2016) and secondary organic aerosol (Prenni et al., 2009; Ignatius et al., 2015) at heterogeneous freezing temperatures is still debated as contradicting results have been observed. Aerosol particles from marine sources are believed to be important INP at remote locations and are subject of current research (Knopf et al., 2011, 2014; DeMott et al., 2015a; Wilson et al., 2015). Recently, also certain minerals have been identified to nucleate ice at temperatures up to 271 K (Harrison et al., 2016). For the implementation of ice nucleation into climate models, a simplistic description of ice formation on different INP types is required. Existing IN parameterizations for dust are typically based either on laboratory experiments using commercially available dusts such as Arizona Test Dust (ATD), or mostly pure clay mineral samples such as illite, kaolinite or montmorillonite (Lüönd et al., 2010; Murray et al., 2011; Niedermeier et al., 2011), dust samples collected from the surface (Niemand et al., 2012) or on in-situ measurements in the atmosphere at locations often distant from major dust sources (DeMott et al., 2010; Tobo et al., 2013). One recent study by DeMott et al. (2015b) combines laboratory data of two surface-collected dust samples with results from two flight campaigns over the Pacific Ocean and the Caribbean Sea within dust layers that underwent long-range transport from Asia and the Sahara respectively. The authors found relatively good agreement between the different samples and concluded that both a parameterization from Niemand et al. (2012) as well as one adapted from Tobo et al. (2013) were applicable for predicting atmospheric mineral dust INP

Atmos. Chem. Phys. Discuss., doi:10.5194/acp-2016-438, 2016
Manuscript under review for journal Atmos. Chem. Phys.
Published: 2 June 2016


Atmospheric Chemistry and Physics Discussions

concentrations.

For laboratory IN experiments, dust samples collected from the surface typically have to be sieved or milled, which may break up larger agglomerates and alter the size-dependent mineralogy (Perlwitz et al., 2015). This could significantly alter the IN ability of these dust particles in laboratory experiments compared to their ambient IN ability. It has been shown that milling of hematite or quartz particles leads to an increase in IN efficiency compared to the unmilled samples (Hiranuma et al., 2014; Zolles et al., 2015). It has been speculated that this is also the reason for ATD, a commercially available dust sample that is washed and milled after collection from a certain desert area in Arizona, being more IN active than natural unprocessed dust samples (Möhler et al., 2006).

Due to their high abundance, for many decades the immersion freezing behavior of atmospheric dust was attributed largely to clay minerals and ice nucleation on relatively pure clay mineral samples were often studied in more detail (Hoffer, 1961; Lüönd et al., 2010; Murray et al., 2010, 2011; Broadley et al., 2012; Pinti et al., 2012; Welti et al., 2012; Hiranuma et al., 2015). Recently, Atkinson et al. (2013) showed that feldspar particles are more efficient immersion mode INP at temperatures above 245 K compared to other minerals. The K-feldspars microcline, orthoclase and sanidine were found to be more IN-active than the Na/Ca-feldspars albite, anorthite and other plagioclase feldspars (Atkinson et al., 2013; Zolles et al., 2015; Peckhaus et al., 2016). Amongst the K-feldspars microcline appears to be the most IN-active (Augustin-Bauditz et al., 2014), even nucleating ice at a temperature of 271 K (Harrison et al., 2016). Feldspars are a highly complex group of minerals and depending on the source region, mineralogically similar samples can have different IN abilities (Harrison et al., 2016). Thus it remains an open question if and how feldspar is affecting the IN behavior of dust in the atmosphere and if it is causing ice nucleation in clouds at $T > 263$ K. Quartz was also found to be more IN-active in the immersion mode than clay minerals but less than the feldspars (Atkinson et al., 2013). It has been proposed that differences in the surface structure can lead to different IN abilities of quartz samples and it is suspected that functional groups on the surface of feldspars and quartz are responsible for their higher IN ability (Zolles et al., 2015). A very recent study by Kaufmann et al. (2016) investigated the IN ability of surface-collected samples from eight different arid regions worldwide and several monomineral reference samples using differential scanning calorimetry. The authors found no significant differences between the surface-collected samples from different source regions. They confirmed the exceptional freezing ability of microcline but found only minor content in two of the natural dust samples studied.

It has been observed that the size distribution and hence mineralogical composition of dust changes during its emission and transport compared to that on the surface (D'Almeida and Schütz, 1983; Murray et al., 2012; Knippertz and Stuut, 2014). The reason for this is a size dependent mineralogical composition caused by differences in the hardness, cleavage and shape of minerals. Hard minerals (e.g. feldspar and quartz) are concentrated in the large grains whereas soft or brittle minerals dominate the small size fraction (e.g. clay minerals). Saltation and hence dust emission strength depends on several factors and is nonlinear in dust particle size (Knippertz and Stuut, 2014). During atmospheric transport, gravitational settling or wet deposition further alters the size distribution.

Airborne dust particles smaller than 20 $\mu$m over the North Pacific have been found to contain 10 to over 50 wt% clay minerals such as illite, kaolinite or smectite, 4 - 40 wt% quartz and 4 - 75 wt% plagioclase feldspar (Leinen et al., 1994). Kandler et al.

Atmos. Chem. Phys. Discuss., doi:10.5194/acp-2016-438, 2016
Manuscript under review for journal Atmos. Chem. Phys.
Published: 2 June 2016


Atmospheric Chemistry and Physics Discussions

(2009) found that dust particles over Morocco consist of about 30 wt% clay minerals (illite, kaolinite, chlorite), less than 5 wt% plagioclase but over 20 wt% K-feldspar, less than 10 wt% quartz and less than 10 wt% calcite in the size range below about 20 $\mu$m geometric diameter. Other identified minerals in the airborne dust were rutile, gypsum, dolomite, hematite or halite. Similar results were found by Falkovich et al. (2001) over Israel. Caquineau et al. (1998) found a north-south gradient of the illite to kaolinite ratio of soil samples in the Sahara with higher values in the northern and western part of the Sahara and lower values in the southern and central Sahara.

In this study we investigate the immersion IN properties of 15 dust samples from nine different deserts around the world. Four of the samples were collected directly from the air (Tenerife) or after deposition from atmospheric transport (Crete, Egypt, Peloponnese) for subsequent analysis in the laboratory without additional treatment such as sieving or milling. All four airborne samples originate from different parts of the Sahara. As part of the Chemistry, Ice Nucleation Efficiency and Mineralogy Of Natural DEsert dust (CINEMONDE) campaign, which took place at ETH Zurich in October and November, 2014, the IN ability of these airborne dusts was investigated and compared to that of several samples collected in the desert. The effect of sieving and milling on the IN behavior of two surface-collected samples was investigated.

Immersion mode IN measurements at temperatures between 235 and 250 K were conducted with the combined set-up of the Zurich Ice Nucleation Chamber, ZINC (Stetzer et al., 2008), and the Immersion Mode Cooling chAmber, IMCA (Lüönd et al., 2010). Particles of four dust samples were collected on filters for subsequent offline analysis with the Frankfurt Ice Deposition Freezing Experiment (FRIDGE) counter operated in the droplet freezing mode as described by Ardon-Dryer and Levin (2014) and Hiranuma et al. (2015). This allowed examination of immersion freezing at temperatures between 250 and 262 K, hence covering a wide range of heterogeneous freezing temperatures. The aim of the current and a follow-up study on deposition/condensation nucleation is to investigate the link between ice nucleation and bulk mineralogy of desert dust as it is found in the atmosphere and to compare it to surface-collected samples. By using aeolian transported samples, the particle size distribution and sample composition are as realistic as possible. To our knowledge this is the first study to investigate IN behavior of airborne desert dust in the laboratory, compare it with surface-collected natural dust samples and link it to the mineralogical composition of these complex samples. With samples from nine different deserts we present a data set covering most major global dust sources.

## 2 Methods

### 2.1 Dust sample origins and processing

The immersion mode freezing behavior of a total of 15 different dust samples was investigated. The collection sites are shown in Fig. 1 together with the major dust emission sources and common atmospheric transport pathways. The GPS coordinates can be found in the supplementary material. It can be seen from Fig. 1 that the dust samples stem from most of the major atmospheric dust sources. The Tenerife sample was collected directly from the air over the course of four days in August 2013 at the Izaña observatory on Tenerife, Spain, using a custom-made large cyclone (Advanced Cyclone Systems, S.A.: flow rate: 200 $m^3h^{-1}$, $D_{50}$ = 1.3 $\mu$m, the diameter at which the collection efficiency is 50 %). After deposition on a roof and on solar

Atmos. Chem. Phys. Discuss., doi:10.5194/acp-2016-438, 2016
Manuscript under review for journal Atmos. Chem. Phys.
Published: 2 June 2016


Atmospheric Chemistry and Physics Discussions

panels, dust samples were collected at the Aburdees observatory, Eygpt on 10 May, 2010 and in Crete and the Peloponnese in Greece in April, 2014. The Crete sample was an integrated sample over several dust events whereas the Peloponnese sample was from one single dust event. Surface collection sites were (i) the Atacama desert in Chile; (ii) a location approximately 70 km from the Uluru in the Australian desert; (iii) the Great Basin in Nevada and (iv) the Mojave desert in California, USA; (v) a Wadi in the Negev desert, approximately 5 km from Sde Boker in Israel; (vi) dunes in the Sahara, close to Merzouga in Morocco; (vii) dunes in the Arabian desert in Dubai; (viii) the Namib in the Etosha National Park in Namibia; and (ix) the Taklamakan desert in China. The Israel sample and the Namib sample are from the same batch as those studied in Kaufmann et al. (2016).

The surface-collected samples needed to be sieved to separate the grain sizes larger than 32 $\mu$m from the remaining sample to avoid clogging of the aerosol generation system used for the IN experiments. Samples were sieved in a cascade of dry sieves with the smallest cut-off size being at 32 $\mu$m diameter (Retsch Vibratory Sieve Shaker AS 200). Typically only a few weight percent of the sample was in this size range. The Australia and Morocco samples had no fraction in this size range and thus were milled using a vibratory disc mill (Retsch, model RS1). For the Atacama and the Israel samples, both a milled and a sieved sample were compared to investigate the effect of milling on ice nucleation. In case of the Atacama sample, part of the unsieved sample was milled. The Israel sample was first sieved and part of the sieved sample with $d \leq 32$ $\mu$m was milled. All natural dust samples are expected to be very heterogeneous, i.e. external and internal mixtures of different minerals and potentially biological material (Meola et al., 2015). Additionally, they have probably undergone natural aging processes due to the exposure to the atmosphere of the surface-collected samples and actual atmospheric aging of the airborne samples (Dall'Osto et al., 2010). This could physically or chemically alter the surface of the dust particles, potentially leading to a coating of the surface and may alter the IN properties compared to the pure mineral dust particles. Effects of washing or heating of the samples, which could yield information on coating or mixing, were not investigated due to the small sample size of the airborne samples.

### 2.2 Dust particle generation

The dust samples were dry dispersed into a 2.78 $m^3$ stainless steel aerosol reservoir tank (Kanji et al., 2013) with a Rotating Brush Generator (RBG, Palas, model RBG 1000) using $N_2$ (5.0) as carrier gas via a cyclone that confined the dust size distribution to below $D_{50}$ = 2.5 $\mu$m. The maximum particle concentration in the tank was about 1200 $cm^{-3}$ and decreased steadily to about 300 $cm^{-3}$ over approximately 10 h. Before each experiment, the tank was cleaned by repeatedly evacuating and purging it with $N_2$ until the particle concentration decreased to 30 - 90 $cm^{-3}$. The total particle concentration was monitored with a Condensation Particle Counter (CPC; TSI model 3772). All instruments sampled directly from the tank. For the IMCA-ZINC measurements the particle concentration was diluted to about 60 $cm^{-3}$ to avoid coincidence effects in the detector.

Atmos. Chem. Phys. Discuss., doi:10.5194/acp-2016-438, 2016
Manuscript under review for journal Atmos. Chem. Phys.
Published: 2 June 2016


Atmospheric Chemistry and Physics Discussions

### 2.3 Aerosol particle size distribution

The particle size distribution in the reservoir tank was monitored over the course of the experiments using a Scanning Mobility Particle Sizer (SMPS; TSI; DMA model 3081, CPC model 3010) for mobility diameters ($d_{\mathrm{m}}$) between 12.2 - 615 nm and an Aerodynamic Particle Sizer (APS; TSI; model 3321) for aerodynamic diameters ($d_{\mathrm{aer}}$) between 0.5 - 20 $\mu$m. After converting the mobility and aerodynamic diameter to volume equivalent diameter ($d_{\mathrm{ve}}$) the size distributions were merged. A shape factor of $\chi$ = 1.36 and a particle density of $\rho$ = 2.65 g cm$^{-3}$ were assumed for the conversion. These values lie in the range of natural dust samples analyzed in earlier studies, e.g. quartz: $\chi$ = 1.10-1.36 (Hinds, 1999; Alexander, 2015), $\rho$ = 2.6 g cm$^{-3}$ (Hinds, 1999; Kandler et al., 2007), illite NX: $\chi$ = 1.49 and $\rho$ = 2.65 g cm$^{-3}$ (Hiranuma et al., 2015). Assuming spherical particles, the area size distribution was calculated and fitted with a bimodal lognormal distribution. The surface area-weighted mean diameter ($\overline{d_{\mathrm{ve,w}}}$) was calculated from the resulting fit for each sample(see Table 1) as well as the surface area corresponding to this weighted average diameter ($\overline{A_{\mathrm{ve,w}}}$). Over the course of a single experiment the size distribution changed as larger particles settle out of the volume faster than smaller ones. This effect was reduced by a fan inside the aerosol tank leading to $\overline{A_{\mathrm{ve,w}}}$ varying by 6 to 24 % over the course of an experiment for the different samples except for the Great Basin sample (64 %).

Figure 2 shows a schematic of the different size fractions resulting from the different collection methods and post-treatment (sieving/ milling) of the samples used for IN experiments in the tank and the mineralogical analysis. Due to the small amount of sample, a mineralogical analysis of the identical size fraction as in the tank ($< 2.5$ $\mu$m) was not possible. Instead, we used the entire size fraction of the airborne samples, the smallest size fraction of the sieved samples ($< 32$ $\mu$m), and for the milled samples, the resulting sizes after milling for the mineralogical analysis.

### 2.4 Mineralogy analysis

The quantitative mineralogical composition of the bulk dust samples was investigated using the X-ray diffraction (XRD)/ Rietveld method (Rietveld, 1969) using a Bragg-Brentano diffractometer (Bruker AXS D8 Advance with CoKalpha-radiation). The qualitative phase composition was determined with the software DIFFRACplus (Bruker AXS). On the basis of the peak position and their relative intensity, the mineral phases were identified in comparison to the Inorganic Crystal Structure Database (Hellenbrandt, 2004). The quantitative composition was calculated by means of Rietveld analysis of the XRD pattern (Rietveld program AutoQuan, GE SEIFERT, Bergmann et al. 1998; Bish and Plötze 2011).

The results and uncertainties for the mineralogy of each sample given from the Rietveld refinement are provided in Tables 2 and 3. For the Egypt sample the mineralogical composition is associated with a significantly higher uncertainty because the amount of sample was small and the measured intensity of the diffracted X-rays very low. In this case the grain statistics was poor and crystals were more likely to be arranged in a certain, preferred direction instead of randomly, leading to a potential overestimation of some mineral fractions. Similarly, the milling of the Israel sample likely interfered with the preferred direction of the minor components in the sieved samples, leading to an observed reduction of these mineral fractions (e.g. illite, kaolinite, plagioclase) in the milled compared to the sieved sample. The differentiation between the microcline and ortho-

Atmos. Chem. Phys. Discuss., doi:10.5194/acp-2016-438, 2016
Manuscript under review for journal Atmos. Chem. Phys.
Published: 2 June 2016


Atmospheric Chemistry and Physics Discussions

clase feldspar (both K-feldspars) fraction was for some samples not possible (i.e. Morocco and Australia) where both phases were likely present. No sanidine feldspar was found in any of the samples. Rietveld fit results for the various Na-plagioclase feldspars (albite, oligoclase and andesine) were often close to being insignificantly different. Hence, they are summarized as Na-plagioclase. The fraction of ankerite and dolomite are usually provided together because in some cases (especially Morocco) it was not possible to differentiate between them. Only for the Namib sample they are provided separately because the fractions were large enough to be distinguishable (Kaufmann et al., 2016).

Due to the broader size range of particles studied with XRD, the mineralogy is not only describing the particles that were studied with the IN chambers but also the fraction between 2.5 - 32 $\mu$m. This could lead to differences between the measured mineralogy and the actual mineralogical composition of particles smaller than 2.5 $\mu$m due to differences in the hardness and cleavage or fracture, i.e. the breaking behavior, of different minerals. This is particularly true for softer minerals such as calcite, which has a Mohs hardness of 3 (standard scale of hardness between 1, talc and 10, diamond), and clay minerals (2 - 2.5) in contrast to feldspars (6) and quartz (7) as well as for minerals with a higher cleavage such as gypsum and calcite (perfect cleavage) compared to quartz (without cleavage, for information on mineral cleavage and hardness see www.mindat.org or www.webmineral.com). Natural mechanical weathering thus likely has enhanced the clay mineral and calcite content in the smaller particle fraction whereas feldspars and quartz tend to be found in the larger size fractions. Since for each filling of the reservoir tank a similar volume of dust sample was used ($\approx$ 0.2 cm$^3$) and the dust density is assumed to be comparable, it can be roughly approximated by the amount of dust sample left over in the 2.5 $\mu$m cut-off cyclone and the particle concentration reached in the tank, what fraction of particles was larger than 2.5 $\mu$m for each sample. Hardly any particles were left over in the cyclone and maximum particle concentrations of 900 - 1200 cm$^{-3}$ were reached by all milled samples apart from the Morocco sample, and by all airborne samples apart from the Egypt sample. Hence, the Atacama and Israel milled, Australia, Crete, Peloponnese and Tenerife samples consisted mainly of particles smaller than 2.5 $\mu$m and the mineralogy is representative for the particles on which ice nucleation was studied. We suspect that the Egypt sample has a higher fraction of large particles because it originated from local sources within Egypt and thus the transport time was much shorter compared to the other airborne samples leading to the size distribution being shifted to larger particles. Of the sieved samples Dubai, Great Basin, Israel, Mojave and Taklamakan, five had a comparably high fraction of particles larger than 2.5 $\mu$m and particle concentrations of 400 - 970 cm$^{-3}$ were reached when filling the tank. Hence, for these samples the presented mineralogy may not be fully representative for the particles investigated for ice nucleation. In contrast, particles of the Namib and Atacama sieved samples were mainly smaller than 2.5 $\mu$m and thus the mineralogy is representative of the small particle fraction. In summary, the identified mineralogical composition is well representative for the particle size fraction used for IN experiments on the Atacama milled and sieved, Israel milled, Australia, Crete, Peloponnese and Tenerife samples.

### 2.5 Immersion freezing experiments and data treatment

Immersion freezing experiments between 235 and 250 K were conducted by extending ZINC (Stetzer et al., 2008) with IMCA (Lüönd et al., 2010). ZINC is a vertically oriented Continuous Flow Diffusion Chamber (Rogers, 1988) with two flat parallel

Atmos. Chem. Phys. Discuss., doi:10.5194/acp-2016-438, 2016
Manuscript under review for journal Atmos. Chem. Phys.
Published: 2 June 2016


Atmospheric Chemistry and Physics Discussions

walls. The walls are ice-coated before an experiment, and by applying a temperature gradient between the two walls at supercooled temperatures, supersaturation with respect to ice is established between the walls. To ensure droplet activation of all sampled particles before freezing, IMCA is installed upstream of ZINC. In IMCA a relative humidity of 120 % with respect to water at a temperature of 303 K is provided by humidified filter paper on the two parallel walls of the chamber. Under these conditions, all particles activate such that each droplet contains a single dust particle. The cloud droplets are then cooled to the experimental IN temperature before they enter ZINC. For the immersion freezing experiments the relative humidity in ZINC is kept at water saturation. The IODE detector (Nicolet et al., 2010) measures the depolarization signal of a linearly polarized laser beam by the particles. This allows differentiation between spherical droplets, which nominally do not lead to a depolarization signal, and the non-spherical ice crystals which depolarize the laser light. The ratio of the detected ice crystal concentration ($N_\mathrm{i}$) to the sum of ice crystals and detected droplet concentration ($N_\mathrm{d}$) is called the frozen fraction ($FF$):

$$FF = \frac{N_\mathrm{i}}{N_\mathrm{d} + N_\mathrm{i}}. \tag{1}$$

IODE can distinguish the depolarization signal of droplets and ice crystals between the limits of detection (LOD) of $FF$ = 0.1 and $FF$ = 0.9. Over the course of about 3 h the temperature is ramped up stepwise. Each data point represents 2000 - 3000 single detected particles.

For subsequent offline immersion freezing measurements between 250 - 263 K with FRIDGE, dust particles were collected by filtration over 3.5 h using Teflon membrane filters (Fluoropore PTFE, 47 mm, 0.2 $\mu$m, Merck Millipore Ltd.). The particles were then extracted from the filters into vials with 10 ml of deionized water for 10 minutes in an ultrasonic bath. 150 drops of 0.5 $\mu$l each were randomly placed on a silicon plate on the cold stage of FRIDGE using an Eppendorff-pipette. At ambient pressure conditions the temperature of the cold stage was then lowered by 1 K min$^{-1}$ and the number of drops freezing as a function of temperature is recorded with a CCD camera. This process is repeated several times with fresh droplets until a minimum of 1000 droplets is exposed. The INP concentration is given by (Vali, 1971; Ardon-Dryer and Levin, 2014)

$$K'(T) = \frac{1}{V_\mathrm{drop}}[\ln(N_0) - \ln(N(T))]\frac{V_\mathrm{water}}{V_\mathrm{air}} \tag{2}$$

where $K'(T)$ is the cumulative INP concentration at a temperature $T$, $V_\mathrm{drop}$ is the volume of a droplet, $N_0$ the number of droplets sampled, $N(T)$ the number of frozen droplets at a temperature $T$, $V_\mathrm{water}$ the volume of water used to wash off the particles from the filter and $V_\mathrm{air}$ the volume of air ($N_2$ in the current study) sampled through the filter. The temperature uncertainty is $\pm$0.2 K and the uncertainty in $FF$ typically $\pm$30 % at $T \leq$260 K and decreases with lower temperatures.

Due to the small sample amounts particularly of the airborne dust samples, generating monodisperse particles for the IN measurements was not possible. To compare the $FF$ measured in IMCA of samples with different size distributions, the $FF$ is normalized by the weighted mean aerosol particle surface area. This yields the ice-active surface site density, $n_\mathrm{s}$:

$$n_\mathrm{s} = -\frac{\ln(1 - FF)}{\overline{A_\mathrm{ve,w}}} \tag{3}$$

In the case of FRIDGE it is calculated as:

$$n_\mathrm{s} = \frac{\ln(1 - \frac{N(T)}{N_0})}{A_\mathrm{t,drop}} \tag{4}$$

Atmos. Chem. Phys. Discuss., doi:10.5194/acp-2016-438, 2016
Manuscript under review for journal Atmos. Chem. Phys.
Published: 2 June 2016


Atmospheric Chemistry and Physics Discussions

with $A_{\mathrm{t,drop}}$ being the total aerosol surface area present in each droplet and given as:

$$A_{\mathrm{t,drop}} = \overline{N} V_{\mathrm{air}} \overline{A_{\mathrm{ve,w}}} \frac{V_{\mathrm{water}}}{V_{\mathrm{drop}}} \tag{5}$$

with the mean total aerosol concentration $\overline{N}$ in the reservoir tank during the time of the particle collection as measured by the CPC. It should be kept in mind that the assumption that $n_{\mathrm{s}}$ stays constant with particle size most likely has limitations for complex polymineral samples such as desert dust particles. Therefore, the provided $n_{\mathrm{s}}$ values should not be treated as an exact parameter, valid at any particle size, but rather a normalization method for the bulk natural dust samples $< 2.5$ $\mu$m which we investigated.

## 3 Results and Discussion

### 3.1 Dust size distribution

Most of the size distributions of the different dust samples in the tank were bimodal. Figure 3 shows exemplary SMPS and APS surface area distribution data of four samples together with the bimodal fit. Since one mode was detected in each instrument's size range, a variation of the shape factor $\chi$ was tested to check if a better overlap of the two size distributions could be achieved. Within realistic limits ($1.1 \leq \chi \leq 1.6$) for shape factors of atmospheric dusts (Alexander, 2015) the two modes remained distinguishable and are thus assumed to be real. Two airborne (Crete and Egypt), one surface-collected sieved and one surface-collected milled (both Israel) samples are shown. The Crete sample has a third small mode at $d_{\mathrm{ve}}$ = 50 nm. Since the smaller aerosol particles contribute only little to the average surface area, the distribution was also bi-modally fitted. The weighted mean particle surface area values are given in Table 1 together with the relative error $\delta(\overline{A_{\mathrm{ve,w}}})$ resulting from a change in distribution during the course of the experiment. All samples peak in number concentration between $d_{\mathrm{ve}}$= 200 - 400 nm and a weighted mean surface area of $\overline{A_{\mathrm{ve,w}}}$ = 2 - 3.7 $\mu$m$^2$ corresponding to a diameter of $\overline{d_{\mathrm{ve,w}}}$=800-1100 nm. Only the Great Basin sample differs strongly because here a minor fraction of particles was smaller than 2.5 $\mu$m leading to a low particle concentration in the reservoir tank and a much higher mean weighted surface area ($\overline{A_{\mathrm{ve,w}}}$ = 16.4 $\mu$m$^2$, $\overline{d_{\mathrm{ve,w}}}$ = 2133 nm). The relative error $\delta(\overline{A_{\mathrm{ve,w}}})$ is 64 % in the case of the Great Basin sample because two refills were necessary during the course of the experiment. For all other samples $\delta(\overline{A_{\mathrm{ve,w}}})$ is less than 24 %. Note that for the Australia sample no SMPS measurements were available due to a technical failure. However, since the surface area mode of all samples lies in the size range of the APS, it is assumed that this is also the case for the Australia sample. Omitting the SMPS data, the average surface area is overestimated since the small particles are missing. As will be discussed in the following, the Australia sample has by far the highest $FF$ and $n_{\mathrm{s}}$ values. If $\overline{A_{\mathrm{ve,w}}}$ was smaller than inferred from measurements only with the APS, it would shift $n_{\mathrm{s}}$ to even higher values thus not affecting the conclusions of our work.

Atmos. Chem. Phys. Discuss., doi:10.5194/acp-2016-438, 2016
Manuscript under review for journal Atmos. Chem. Phys.
Published: 2 June 2016


Atmospheric Chemistry and Physics Discussions

### 3.2 Ice nucleation of desert dust

The plots on the left side of Fig. 4 show the $FF$ as a function of temperature between 235 and 253 K, separately for non-Saharan and the Saharan samples. The homogeneous freezing regime is indicated in light gray and the LOD of IMCA in dark gray bands. The majority of the non-Saharan $FF$ curves (Fig. 4a and b) behave similarly, with two samples being distinctly different: the Australia sample shows significantly higher $FF$ values at all temperatures whereas the milled Israel sample falls clearly below the other $FF$ curves for all $T > 237$ K. Of the intermediately active samples, the Taklamakan and Great Basin samples are at the upper end whereas the Dubai sample shows the second lowest $FF$ values. The remaining samples are mostly not significantly different, with $FF$ values lying within each others error bars.

The five Saharan samples in Fig. 4c cover a comparable range of $FF$ at any temperature as the non-Saharan ones. The only surface-collected Saharan sample (Morocco) has higher $FF$ values compared to the airborne Saharan samples. All samples were fit with sigmoidal curves. None of the samples shows a stepwise $FF$ owing to the polydisperse size distribution of the particles. Due to the polymineral nature of the samples a stepwise activation of the different mineral species could be expected with decreasing temperature if the single mineral components were externally mixed and not present within one particle. Since IN activity is also dependent on the surface area of each particle (Archuleta et al., 2005; Connolly et al., 2009; Welti et al., 2009), larger particles will activate at higher temperatures than smaller ones, smoothing out the potential step function of different minerals.

$n_s$ was calculated from the $FF$ using $\overline{A_{ve,w}}$ in Eq. 3 to account for differences in the size distributions which may impact the IN behavior. The results are shown in the plots on the right side of Fig. 4. The error bars in $n_s$ are derived by error propagation from the error in $FF$ and $\delta(\overline{A_{ve,w}})$. Data points outside of $0.1 < FF < 0.9$ and in the homogeneous freezing regime are omitted. The $n_s$ of the Australian sample remains the highest of all samples and that of the Israel milled sample one of the lowest together with that of the Great Basin sample. Among the Saharan samples (Fig. 4f), the $n_s$ of the Tenerife sample is similar to that of Crete, whereas the Egypt sample is higher for $T > 238$ K. The $n_s$ of the surface-collected and milled Morocco sample is distinctly higher at all temperatures.

To compare all dust samples, the $n_s$ in $m^{-2}$ was fitted using the exponential function:

$$n_s(m^{-2}) = \exp(-a(T - 273.15K) + b) \quad (6)$$

with the fit parameters $a$ and $b$, which are given in Table 4 for each sample. The resulting fit lines from all samples are shown in Fig. 5a. Overall the Australian sample is by far the most IN active sample. The Israel milled and the Peloponnese sample show a low IN activity. Overall, the airborne Saharan samples belong to the lower half of all $n_s$ curves. As a consequence of the large mean surface area of the Great Basin sample its $n_s$ is shifted to the lowest values. The $n_s$ fits for K-feldspar from Atkinson et al. (2013), for kaolinite KGb-1b from Murray et al. (2011), for Illite NX from Broadley et al. (2012) and the $n_s$ parameterization curve from Niemand et al. (2012) are shown for comparison. The first three are based on droplet freezing experiments with droplets much larger ($d$ = 8-52 $\mu$m) than in IMCA, each containing a higher dust surface area per droplet (9.06 $10^{-12}$ to 2.77 $10^{-8}$ $m^2$). Thus, they are limited to lower $n_s$ values than those from IMCA. It can be seen that all desert dust samples fall between the K-feldspar and the clay mineral fits at all temperatures. The parameterization from Niemand et al.

Atmos. Chem. Phys. Discuss., doi:10.5194/acp-2016-438, 2016
Manuscript under review for journal Atmos. Chem. Phys.
Published: 2 June 2016


Atmospheric Chemistry and Physics Discussions

(2012) was also based on the $n_s(T)$ of three polydisperse surface-collected dust samples from China, Egypt and the Canary Islands and one sample collected after deposition in Israel. The comparison to our broader collection of global surface-collected and airborne dust samples shows that the parameterization falls in the same range of $n_s$ but rather at the lower end. Given that the measurements were conducted with different instruments, which can lead to a systematic offset of up to three orders of magnitude in terms of $n_s$ as shown by Hiranuma et al. (2015), and the polydisperse nature of the dust samples, the agreement is considered reasonable. The maximum difference in temperature between the parameterization from Niemand et al. (2012) and the average of all $n_s$ curves from this study (not shown) is less than 3 K, while the spread in $n_s$ curves across all samples in our study is up to 10 K. The parameterization captures well the temperature dependence of the Israel sieved sample and has a slope close to that of all airborne samples. Interestingly, most of the surface-collected samples show a more moderate slope, i.e. a lower temperature dependence.

The high temperature measurements from FRIDGE are shown in Fig. 5b together with those from IMCA and parameterizations. Again, the desert dusts fall between the (extrapolations) of the clay mineral and K-feldspar fits. The parameterization from Niemand et al. (2012) overpredicts most of the $n_s$ measured by FRIDGE by an order of magnitude apart from the Atacama milled sample at $T$ = 251 - 256 K where the parameterization overpredicts the measurements only by about 30 %. At temperatures above 250 K the milled Atacama dust is by far the most ice-active of the four studied samples. This is in contrast to the observations at $T < 245$ K where the Atacama milled sample is slightly less ice-active than the Taklamakan sample (see Fig. 5a). Generally, it can be seen from comparing the IMCA data to the FRIDGE data that there are differences in the relative order of IN activity as a function of temperature. The fits of $n_s$(T) are thus not the same over the whole temperature range and are only valid for the given range. The potential effects of mineralogy on the IN activity at different temperatures is investigated in the following section.

### 3.3 Role of mineralogy

Various earlier studies have shown that the IN activity expressed by $n_s$ varies by several orders of magnitude between different types of minerals. Tables 2 and 3 show the results of the mineralogical analysis of the dust samples. Note that the mineralogical composition of the Namib sample was taken from Kaufmann et al. (2016). The distinct composition of the Australia sample is striking. In contrast to all other samples it consists almost entirely of quartz (91.3 wt%) and K-feldspars (8.1 wt%) which are highly ice-active minerals in the immersion mode (Atkinson et al., 2013; Zolles et al., 2015). Also the Morocco sample has a high quartz content (63.8 wt%) which is followed by the Taklamakan sample (33.1 wt%), both also belonging to the highest ice-active samples of this study. The remaining samples have a quartz content of 23 wt% or less. Another obvious difference is the high feldspar content of both Atacama samples (milled: 22.3 wt% orthoclase, 43.2 wt% Na-plagioclase, sieved: 11.8 wt% orthoclase, 39.3 wt% Na-plagioclase). The milled Atacama sample shows the highest $n_s$ of the four investigated samples in FRIDGE at $T$ >250 K (Fig. 5b), close to the K-feldspar parameterisation by Atkinson et al. (2013) at 260 < $T$ < 262 K and also higher activities than the sieved sample at $T > 240$ K (Fig. 6). The Israel samples have a distinctly high calcite content (milled: 81 wt%, sieved: 67.2 wt%), followed by Dubai (37.2 wt%) and Peloponnese (33 wt%). Calcite has been found to be

Atmos. Chem. Phys. Discuss., doi:10.5194/acp-2016-438, 2016
Manuscript under review for journal Atmos. Chem. Phys.
Published: 2 June 2016


Atmospheric Chemistry and Physics Discussions

a weakly ice-active mineral in the immersion mode (Atkinson et al., 2013; Zolles et al., 2015) and also in the condensation mode (Roberts and Hallett, 1969; Zimmermann et al., 2008). The Namib sample consists of about one quarter each of calcite (29 wt%), dolomite (27 wt%) and ankerite (23 wt%) and 10 wt% muscovite but no significant fraction of clay minerals, feldspars or quartz (1 wt% smectite and 1 wt% quartz were identified). This is surprising because the Namib sample is one the most IN-active samples at $T < 242$ K. The IN ability of the mica muscovite is debated as some studies have found hardly any IN activity at heterogeneous freezing temperatures (Atkinson et al., 2013; Campbell et al., 2015; Kaufmann et al., 2016) while others found significant IN ability at $T < 243$ K (Steinke, 2013; Abdelmonem et al., 2015). Kaufmann et al. (2016) found little IN activity of a reference dolomite sample. No study so far has investigated the IN behavior of pure ankerite. Thus it remains unclear what leads to the observed high IN acitivity at $T < 242$ K of the Namib sample.

The remaining samples are more complex mixtures of quartz, feldspars, clay minerals, micas and other minerals. We find microcline in at least three of the surface-collected (Great Basin and both Israel) and also in the airborne Tenerife sample. In the samples from Australia and Morocco both phases orthoclase and microcline seem to be present.

The Saharan samples show a great variety with the Tenerife sample having the highest content of clay minerals (illite + kaolinite + palygorskite: 43.3 wt%) of all dusts very similar to the findings of Alastuey et al. (2005). The other airborne Saharan samples (Egypt, Peloponnese and Crete) consist to about 50 wt% of quartz and calcite. This is likely due to different source regions within the Sahara. Based on air mass back trajectory calculations the Tenerife sample originated in Northern Mauritania or Morocco, whereas the Egypt sample stemmed from local sources in Egypt and the Peloponnese and Crete samples from Northern Saharan sources in Algeria, Tunisia and Lybia. The large discrepancy between the Morocco and Tenerife sample furthermore shows that even if the source region of an airborne sample can roughly be localized, the mineralogy of surface-based and airborne samples can differ. Schütz and Sebert (1987) found that the mineral composition of the size fraction $<5$ $\mu$m of surface-collected samples in the Sahara was very similar throughout the Sahara and concluded that this size fraction is already well mixed within the desert. The main differences were a higher calcite and palygorskite content in the Northern Sahara which is consistent with our findings for the Egypt, Peloponnese and Crete samples in the case of calcite. We find comparable amounts of palygorskite in the Crete, Peloponnese and Tenerife samples (4.5 - 5.3 wt%) but no palygorskite in the Egypt and Morocco sample. The differences with regard to mineralogical composition and IN ability found between the Morocco (higher quartz content) and the Tenerife (higher clay mineral content) sample suggests that surface-collected samples are not necessarily representative for the airborne dust aerosol even if originating from the same region. This is supported by the fact that the Morocco sample consisted mostly of dust grains larger than 32 $\mu$m which sediment quickly before being transported long distances in the atmosphere.

In the following we investigate how much of the differences in $n_s$ between the dust samples can be attributed to their mineralogy. For this, we compare the fraction of single minerals to the $n_s$ of our dust samples at five different temperatures. We choose mineral phases which have been found to have $n_s$ values in a range which is measurable with IMCA (Atkinson et al., 2013; Hiranuma et al., 2015; Zolles et al., 2015; Harrison et al., 2016; Peckhaus et al., 2016). Additionally, we compare the following sums of minerals to the samples' $n_s$: K-feldspars (microcline and orthoclase) ; all feldspars (K-feldspars plus Na-plagioclase feldspars); sum of all feldspars plus quartz; sum of all feldspars plus quartz plus illite and/or kaolinite. We do not differentiate

Atmos. Chem. Phys. Discuss., doi:10.5194/acp-2016-438, 2016
Manuscript under review for journal Atmos. Chem. Phys.
Published: 2 June 2016


Atmospheric Chemistry and Physics Discussions

between the different feldspar polymorphs because even the same type of feldspar can vary in $n_s$ as shown by Harrison et al. (2016) due to the complex structure of feldspars. The Namib sample was excluded from the correlations with feldspars, quartz and clays because it does not contain any significant amount of these minerals. However, it was included for the comparison with calcite.

The first six columns in Table 5 show the Pearson correlation coefficients ($R$) between the mineral fractions and the $n_s$ at five temperatures. At 253 K only three samples (Atacama milled, Egypt and Taklamakan) are available for comparison. For these, the K-feldspar content leads to a very high correlation ($R$ = 0.99) and adding the Na-plagioclase to the feldspar sum reduces the R value to 0.93. At lower temperatures, no significant correlation is found between the K-feldspar content and $n_s$. At 245 K, the $n_s$ correlates best ($R$ = 0.91) with the quartz alone and adding of feldspar, illite or kaolinite leads to a lower $R$ value (0.73 - 0.78). This is in agreement with earlier studies showing the comparable high immersion mode IN activity of quartz at this temperature (Atkinson et al., 2013; Zolles et al., 2015). Interestingly, this behavior stays the same at 243 K ($R$ = 0.92) and 240 K ($R$ = 0.80). Only at 238 K adding feldspars and kaolinite to the quartz improves the correlation slightly (from $R$ = 0.60 to 0.64 and 0.61, respectively). Note that the Australia sample, which has the highest quartz content, is excluded at 240 K and 238 K from the correlation analysis because $FF > 0.9$. Illite alone shows a weak anticorrelation with $n_s$ at any of the investigated temperatures and leads to reduced or constant $R$ values when added to the quartz plus feldspar sum. Also calcite and kaolinite are anticorrelated with $n_s$ at all presented temperatures. This means that a higher IN activity in one sample can be attributed at 253 K to the K-feldspar content present in this sample whereas at temperatures between 238 - 245 K it is attributed to the sum of feldspar and quartz content present. A high clay mineral content on the other hand is associated with a lower IN activity of a sample.

These results need to be treated carefully because the mineralogy is derived for the full size range up to 32 $\mu$m and may be different in the size fraction $<$ 2.5 $\mu$m studied with regard to ice nucleation. Therefore, we do the same analysis exclusively for the samples for which the size fraction larger than 2.5 $\mu$m was small and the mineralogical composition determined by XRD can be assumed to be representative for particles $<$ 2.5 $\mu$m. These samples are: Atacama milled and sieved, Australia, Crete, Peloponnese, Israel milled and Tenerife. From these samples only the IN ability of the Atacama milled sample was measured with FRIDGE at 253 K and only two of the samples show measurable $n_s$ at 245 K in the IMCA data, thus those temperatures are excluded. The results for 243 K, 240 K, and 238 K are given in the last three columns of Table 5. At 243 K quartz and the sum of all feldspars show both the highest $R$ value (0.99) for the selected samples. At 240 K and 238 K the sum of all feldspars ($R$ = 0.99 and $R$ = 0.92, respectively) and the sum of all feldspars plus quartz ($R$ = 0.97 and $R$ = 0.93, respectively) show the highest correlation with $n_s$. This is different to the finding from above when all samples were included and quartz exclusively led to the highest $R$ values. The difference stems mainly from the exclusion of the Morocco, Taklamakan, Egypt and Great Basin samples, which all had a high quartz content. It is noteworthy that the correlation with illite and kaolinite is still negative at any temperature despite the fact that some of the analyzed samples contain a comparably large amount of clay minerals (Tenerife: 38.5 wt%, Peloponnese: 20.2 wt%).

In summary these results are in contrast to the assumption that clay minerals such as illite and kaolinite are the main drivers of ice nucleation of desert dust. Our study supports findings that quartz and feldspars are more IN-active in the immersion

Atmos. Chem. Phys. Discuss., doi:10.5194/acp-2016-438, 2016
Manuscript under review for journal Atmos. Chem. Phys.
Published: 2 June 2016




mode than clay minerals also at low heterogeneous freezing temperatures. The results further show that at temperatures above 250 K the K-feldspar content determines the IN behavior while below 245 K, Na-plagioclase feldspars and quartz are of similar importance. We confirmed this trend for the size fraction smaller than 2.5 $\mu$m where clay minerals are likely enriched and the mineralogy is representative for the size fraction on which ice nucleation was studied. This size fraction is of particular interest for atmospheric ice nucleation studies as it is most relevant for long-range transport and atmospheric advection to altitudes relevant to ice cloud formation. We find microcline in some of our natural dust samples and also in one of the airborne samples. However, we cannot confirm a superior role of microcline over orthoclase for ice nucleation as in most samples microcline was found to be less than 8 wt%. The Great Basin sample contained 30 wt% microcline in the bulk sample but likely significantly less in the size fraction $< 2.5$ $\mu$m. The highly polymineral nature of our samples and the effect of differences in the size distributions prevent a further investigation of the role of microcline.

It should be noted that XRD is a bulk analysis of the mineralogical composition whereas ice nucleation is most likely a process sensitive to the surface or the first few layers below the surface in case of an ice germ growing out of cracks, crevices or pores (Marcolli, 2014; Welti et al., 2014). Despite this difference in sensitivity, a high correlation between bulk mineralogy and IN activity is found in this study. XRD also does not allow any inference of the mixing state of different minerals at a certain size. Hence we do not know, particularly for the small particles, if each particle contains some amount of quartz and/or feldspar or if pure calcite or clay mineral particles exist. However, our results indicate that any feldspar or quartz present in the bulk dust will dominate its freezing behavior down to low heterogeneous freezing temperatures. The results suggest that potential coating of the particles only plays a secondary role for the immersion freezing ability of the mineral dusts as the majority of the results can be explained by the mineralogy as has also been observed by Kaufmann et al. (2016). This may be due to a significant dilution of coating material in the droplets forming on each dust particle and may have a more prominent role in deposition nucleation. The only sample where the IN behavior remains inconclusive with respect to its mineralogy is the Namib sample. If this is due to reasons other than mineralogy such as coating as suggested by Kaufmann et al. (2016) or if the present minerals ankerite, dolomite or muscovite can lead to a high IN activity at $T < 243$ K under certain circumstances is not known.

### 3.4 Effect of milling

Two of the dust samples have undergone two different treatments (sieving and milling) to compare the effect of milling on $n_s$ of a polymineral sample. The Israel sample was first sieved and then part of the $d \leq 32$ $\mu$m fraction was milled. For the Atacama sample, the original sample containing particles of all sizes was split, one part was sieved and one part milled. The resulting $n_s$ curves are shown in Fig. 6. Interestingly, the two sieved samples are very similar in $n_s$. The milling of the Atacama sample led to a slightly higher IN efficiency at $T > 240$ K compared to the sieved sample. Contrastingly, in case of the Israel sample milling led to a strong decrease in $n_s$ at all studied temperatures. The latter could be related to the high calcite content of the Israel dust. Calcite is a rather soft mineral with a Mohs hardness of 3 and a perfect cleavage, and during the milling process it could be ground faster to a smaller grain size compared to harder minerals such as quartz (Mohs hardness of 7) or feldspar (6). Thus it would be persistent in the size fraction $d_{ve} \leq 2.5$ $\mu$m. Calcite has been found to be ice-active only very

Atmos. Chem. Phys. Discuss., doi:10.5194/acp-2016-438, 2016
Manuscript under review for journal Atmos. Chem. Phys.
Published: 2 June 2016


Atmospheric Chemistry and Physics Discussions

close to the homogeneous freezing regime (Atkinson et al., 2013; Zolles et al., 2015) and anticorrelated with $n_s$ at all presented temperatures in this study (Table 5). Similarly, the slightly higher $n_s$ at $T > 240$ K of the milled Atacama sample is likely due to more feldspar being present in the $d_{ve} > 32$ $\mu$m fraction, which then got milled into sizes $d_{ve} < 2.5\mu$m, compared to the sieved sample. It can be seen from Tables 2 and 3 that the K-feldspar (orthoclase) content is higher in the Atacama milled sample (22 wt%) than in the sieved one (12 wt%). The milled sample mostly consisted of particles smaller than 2.5 $\mu$m, whereas the sieved one had a large fraction of particles larger than 2.5 $\mu$m. Thus, there was likely more orthoclase content in the milled Atacama sample particles smaller than 2.5 $\mu$m compared to those in the sieved sample, leading to higher $n_s$ at warmer temperatures. Effects such as an increase in surface irregularities, defect density and functional groups due to the milling as reported by other authors (Hiranuma et al., 2014; Zolles et al., 2015) are not excluded but were not investigated in this study. However, an increase in defect density and surface irregularities has been shown to increase the IN activity of monomineral or single compound samples. Thus, we conclude for the Israel sample that a morphology effect is small in comparison to the change in mineralogical composition caused by the milling in the analyzed size range. This re-emphasizes the importance of mineralogy for the surface sensitive IN process.

## 4 Conclusions

The IN ability in the immersion mode of 15 natural desert dust samples was quantified by the frozen fraction and the ice-active surface site density and compared with the bulk dust sample mineralogy. A diverse mineralogical composition was found for the different desert dust samples which related to variable IN abilities. The comparison showed that at temperatures above 250 K the highest $FF$ and $n_s$ are related to the highest fraction of K-feldspars in the sample. At temperatures below 250 K on the other hand, the IN ability can mainly be attributed to the quartz content of the samples as well as to the sum of all feldspars (K-feldspars and Na-plagioclase feldspars). The clay mineral (illite and kaolinite) and calcite content of the dust samples was negatively correlated with their $n_s$ at all studied temperatures. These results show that natural desert dust's IN ability above 253 K can mainly be attributed to the presence of K-feldspar in the dust. Moreover our study stresses the important role of quartz and all feldspars for the IN behavior of desert dust at heterogeneous freezing temperatures below 250 K and shows that clay minerals are of minor importance to predicting the IN activity of natural dust samples in the immersion mode if quartz or feldspar are present.

The size dependent enrichment of different minerals leading to differences in $n_s$ highlights the interplay between IN ability and atmospheric relevance of certain mineral phases. The most IN-active minerals quartz and feldspars are also among the hardest minerals while the less IN-active clay minerals and calcite are softer minerals. The focus of earlier IN studies on the clay mineral IN behavior is supported by the observation that three of the four airborne samples (Crete, Peloponnese and Tenerife), which had been long-range transported and were almost entirely in the size range $< 2.5$ $\mu$m, had the highest clay mineral fraction. These samples as well as the surface-collected and sieved Mojave sample were amongst the least IN-active samples. Quartz is a comparably hard mineral and thus less common in the smallest dust size fractions. Since we measured IN activity

Atmos. Chem. Phys. Discuss., doi:10.5194/acp-2016-438, 2016
Manuscript under review for journal Atmos. Chem. Phys.
Published: 2 June 2016


Atmospheric Chemistry and Physics Discussions

of particles smaller than 2.5 $\mu$m and found a high correlation with the quartz content of the dust samples we show that quartz is nevertheless an important atmospheric INP component. Milling of dust samples in the laboratory or mechanical weathering processes in nature cannot only lead to more surface inhomogeneities but also to an enrichment of more IN-active minerals such as quartz in sizes relevant for atmospheric ice nucleation. Potentially this also explains the higher IN activity of Arizona test dust compared to other desert dust samples which was found in multiple earlier studies (Möhler et al., 2006; Zolles et al., 2015; Kaufmann et al., 2016). Thus, mechanical weathering of dust particles on the surface plays a crucial role in determining the mineralogical composition of those particles that get emitted into the air, transported over long distances and potentially involved in cloud microphysical processes. The observed differences between the surface-collected Morocco sample and the airborne Tenerife sample stemming from Mauritania or Morocco stresses that surface-collected samples are not necessarily representative for those transported over long distances. Thus, more IN studies on airborne, transported dust are crucial to quantify the ability of atmospheric dust to nucleate ice. Furthermore, if airborne dust is generally found to be less IN-active than surface-collected dust and does not show IN activity at temperatures above 263 K, it can not explain first ice formation in clouds with top temperatures warmer than 263 K. For that other INP such as biological particles or different mechanisms such as seeder - feeder processes would need to be investigated.

The applicability of the parameterization by Niemand et al. (2012) to describe an average IN behavior of desert dust was confirmed by a global set of dust samples. However, the variation between the different samples in temperature for a certain frozen fraction was up to 9 K and up to 10 K when considering $n_s$. To more adequately describe immersion freezing by desert dust in the atmosphere, mineralogy sensitive emission and transport schemes would be desirable. Hereby, the K-feldspar for temperatures above 250 K and at lower temperatures additionally also Na-plagioclase feldspars and quartz emissions and transport should be quantified. Since this is complex and computationally expensive, more studies quantifying the IN ability of dust as it is found in the atmosphere may circumvent this approach. To our knowledge this is the first time that the IN ability of airborne dust as well as surface-collected dust samples was quantified and explained by the dust mineralogy.

*Author contributions.* YB collected the Tenerife and Israel samples, initiated, planned and lead CINEMONDE, performed and analyzed the XRD measurements, analyzed the IN and aerosol data and wrote the manuscript, AW, JA and FR conducted the IMCA measurements, AW analyzed the IMCA data and collected the Australia, Mojave and Great Basin sample, AD performed the FRIDGE sample collection and analysis, HB supervised the FRIDGE data analysis and contributed to the manuscript, MP performed and analyzed the XRD measurements, BS, ZAK and UL supervised the project and contributed to the manuscript.

*Acknowledgements.* The various dust samples in this paper have been collected by a number of people who the authors are very thankful to: Maria Kanakidou and her team (Peloponnese, Crete), Felix Lüönd (Atacama), Paolo D'Odorico and Christopher Hoyle (Namib), Lukas Kaufmann (Taklamakan), Monika Kohn (Dubai), Joel Corbin (Morocco), Sergio Rodríguez and unknown Egyptian researchers (Egypt). Furthermore, we thank the rest of the CINEMONDE team: Annika Kube, Larissa Lacher and Fabian Mahrt, as well as Hannes Wydler

Atmos. Chem. Phys. Discuss., doi:10.5194/acp-2016-438, 2016
Manuscript under review for journal Atmos. Chem. Phys.
Published: 2 June 2016


for technical support. Y. Boose is funded by the Swiss National Science Foundation (grant 200020 150169/1). AD and HB gratefully acknowledge support by Deutsche Forschungsgemeinschaft (DFG) under the Research Unit FOR 1525 (INUIT).

Atmos. Chem. Phys. Discuss., doi:10.5194/acp-2016-438, 2016
Manuscript under review for journal Atmos. Chem. Phys.
Published: 2 June 2016




## References

Abdelmonem, A., Lützenkirchen, J., and Leisner, T.: Probing ice-nucleation processes on the molecular level using second harmonic generation spectroscopy, Atmos. Meas. Tech., 8, 3519–3526, doi:10.5194/amt-8-3519-2015, 2015.

Alastuey, A., Querol, X., Castillo, S., Escudero, M., Avila, A., Cuevas, E., Torres, C., Romero, P.-M., Exposito, F., García, Diaz, J., Van Dingenen, R., and Putaud, J. P.: Characterisation of TSP and PM2.5 at Izaña and Sta. Cruz de Tenerife (Canary Islands, Spain) during a Saharan Dust Episode (July 2002) , Atmos. Environ., 39, 4715 – 4728, doi:10.1016/j.atmosenv.2005.04.018, 2005.

Alexander, J. M.: Optical properties of mineral dust aerosol including analysis of particle size, composition, and shape effects, and the impact of physical and chemical processing, Ph.D. thesis, University of Iowa, 2015.

Archuleta, C., DeMott, P., and Kreidenweis, S.: Ice nucleation by surrogates for atmospheric mineral dust and mineral dust/sulfate particles at cirrus temperatures, Atmos. Chem. Phys., 5, 2617–2634, doi:1680-7324/acp/2005-5-2617, 2005.

Ardon-Dryer, K. and Levin, Z.: Ground-based measurements of immersion freezing in the eastern Mediterranean, Atmos. Chem. Phys., 14, 5217–5231, doi:10.5194/acp-14-5217-2014, 2014.

Atkinson, J., Murray, B. J., Woodhouse, M. T., Whale, T. F., Baustian, K. J., Carslaw, K. S., Dobbie, S., O'Sullivan, D., and Malkin, T. L.: The importance of feldspar for ice nucleation by mineral dust in mixed-phase clouds, Nature, 498, 355 – 358, doi:10.1038/nature12278, 2013.

Augustin-Bauditz, S., Wex, H., Kanter, S., Ebert, M., Niedermeier, D., Stolz, F., Prager, A., and Stratmann, F.: The immersion mode ice nucleation behavior of mineral dusts: A comparison of different pure and surface modified dusts, Geophys. Res. Lett., 41, 1–8, doi:10.1002/2014GL061317, 2014.

Bergmann, J., Friedel, P., and Kleeberg, R.: BGMN - a new fundamental parameters based Rietveld program for laboratory X-ray sources, it's use in quantitative analysis and structure investigations., Commission of Powder Diffraction, International Union of Crystallography CPD Newslett., 20, 5–8, 1998.

Bish, D. L. and Plötze, M.: X-ray powder diffraction with emphasis on qualitative and quantitative analysis in industrial mineralogy, in: Industrial Mineralogy, EMU Notes in Mineralogy, edited by Christidis, G., vol. 9, chap. 3, pp. 35–76, 2011.

Boose, Y., Kanji, Z. A., Kohn, M., Sierau, B., Zipori, A., Crawford, I., Lloyd, G., Bukowiecki, N., Herrmann, E., Kupiszewski, P., Steinbacher, M., and Lohmann, U.: Ice Nucleating Particle Measurements at 241 K during Winter Months at 3580 MSL in the Swiss Alps, J. Atmos. Sci., 73, 2203–2228, doi:10.1175/JAS-D-15-0236.1, 2016a.

Boose, Y., Sierau, B., García, M. I., Rodríguez, S., Alastuey, A., Linke, C., Schnaiter, M., Kupiszewski, P., Kanji, Z. A., and Lohmann, U.: Ice nucleating particles in the Saharan Air Layer, Atmos. Chem. Phys. Discuss., doi:10.5194/acp-2016-192, in review, 2016b.

Boucher, O., Randall, D., Artaxo, P., Bretherton, C., Feingold, G., Forster, P., Kerminen, V.-M., Kondo, Y., Liao, H., Lohmann, U., Rasch, P., Satheesh, S., Sherwood, S., Stevens, B., and Zhang, X.: Clouds and Aerosols. In: Climate Change 2013: The Physical Science Basis. Contribution of Working Group I to the Fifth Assessment Report of the Intergovernmental Panel on Climate Change, Cambridge University Press, Cambridge, United Kingdom and New York, NY, USA., [Stocker, T.F., D. Qin, G.-K. Plattner, M. Tignor, S.K. Allen, J. Boschung, A. Nauels, Y. Xia, V. Bex and P.M. Midgley (eds.)]., 2013.

Broadley, S. L., Murray, B. J., Herbert, R. J., Atkinson, J. D., Dobbie, S., Malkin, T. L., Condliffe, E., and Neve, L.: Immersion mode heterogeneous ice nucleation by an illite rich powder representative of atmospheric mineral dust, Atmos. Chem. Phys., 12, 287–307, doi:10.5194/acp-12-287-2012, 2012.



Brooks, S. D., Suter, K., and Olivarez, L.: Effects of Chemical Aging on the Ice Nucleation Activity of Soot and Polycyclic Aromatic Hydrocarbon Aerosols, J. Phys. Chem. A, 118, 10 036–10 047, doi:10.1021/jp508809y, pMID: 25280086, 2014.

Campbell, J. M., Meldrum, F. C., and Christenson, H. K.: Is Ice Nucleation from Supercooled Water Insensitive to Surface Roughness?, J. Phys. Chem. C, 119, 1164–1169, doi:10.1021/jp5113729, 2015.

Caquineau, S., Gaudichet, A., Gomes, L., Magonthier, M.-C., and Chatenet, B.: Saharan dust: Clay ratio as a relevant tracer to assess the origin of soil-derived aerosols, Geophys. Res. Lett., 25, 983–986, doi:10.1029/98GL00569, 1998.

Chou, C., Stetzer, O., Weingartner, E., Jurányi, Z., Kanji, Z. A., and Lohmann, U.: Ice nuclei properties within a Saharan dust event at the Jungfraujoch in the Swiss Alps, Atmos. Chem. Phys., 11, 4725–4738, doi:10.5194/acp-11-4725-2011, 2011.

Connolly, P., Möhler, O., Field, P., Saathoff, H., Burgess, R., Choularton, T., and Gallagher, M.: Studies of heterogeneous freezing by three different desert dust samples, Atmos. Chem. Phys., 9, 2805–2824, doi:10.5194/acp-9-2805-2009, 2009.

Dall'Osto, M., Harrison, R. M., Highwood, E. J., O'Dowd, C., Ceburnis, D., Querol, X., and Achterberg, E. P.: Variation of the mixing state of Saharan dust particles with atmospheric transport, Atmos. Environ., 44, 3135–3146, doi:10.1016/j.atmosenv.2010.05.030, 2010.

D'Almeida, G. A. and Schütz, L.: Number, Mass and Volume Distributions of Mineral Aerosol and Soils of the Sahara, J. Climate Appl. Meteor., 22, 233–243, doi:10.1175/1520-0450(1983)022<0233:NMAVDO>2.0.CO;2, 1983.

DeMott, P. J., Sassen, K., Poellot, M., Baumgardner, D., Rogers, D., Brooks, S., Prenni, A., and Kreidenweis, S.: African dust aerosols as atmospheric ice nuclei, Geophys. Res. Lett., 30, 1732, doi:10.1029/2003GL017410, 2003, 2003.

DeMott, P. J., Prenni, A. J., Liu, X., Kreidenweis, S. M., Petters, M. D., Twohy, C. H., Richardson, M. S., Eidhammer, T., and Rogers, D. C.: Predicting global atmospheric ice nuclei distributions and their impacts on climate, Proc. Natl. Acad. Sci., 107, 11 217–11 222, doi:10.1073/pnas.0910818107, 2010.

DeMott, P. J., Hill, T. C. J., McCluskey, C. S., Prather, K. A., Collins, D. B., Sullivan, R. C., Ruppel, M. J., Mason, R. H., Irish, V. E., Lee, T., Hwang, C. Y., Rhee, T. S., Snider, J. R., McMeeking, G. R., Dhaniyala, S., Lewis, E. R., Wentzell, J. J. B., Abbatt, J., Lee, C., Sultana, C. M., Ault, A. P., Axson, J. L., Diaz Martinez, M., Venero, I., Santos-Figueroa, G., Stokes, M. D., Deane, G. B., Mayol-Bracero, O. L., Grassian, V. H., Bertram, T. H., Bertram, A. K., Moffett, B. F., and Franc, G. D.: Sea spray aerosol as a unique source of ice nucleating particles, Proc Natl Acad Sci, doi:10.1073/pnas.1514034112, 2015a.

DeMott, P. J., Prenni, A. J., McMeeking, G. R., Sullivan, A. P., Petters, M. D., Tobo, Y., Niemand, M., Möhler, O., Snider, J. R., Wang, Z., and Kreidenweis, S. M.: Integrating laboratory and field data to quantify the immersion freezing ice nucleation activity of mineral dust particles, Atmos. Chem. Phys., 15, 393–409, doi:10.5194/acp-15-393-2015, 2015b.

Falkovich, A. H., Ganor, E., Levin, Z., Formenti, P., and Rudich, Y.: Chemical and mineralogical analysis of individual mineral dust particles, J. Geophys. Res. Atmos., 106, 18 029, doi:10.1029/2000JD900430, 2001.

Harrison, A. D., Whale, T. F., Carpenter, M. A., Holden, M. A., Neve, L., O'Sullivan, D., Vergara Temprado, J., and Murray, B. J.: Not all feldspar is equal: a survey of ice nucleating properties across the feldspar group of minerals, Atmos. Chem. Phys. Discuss., 2016, 1–26, doi:10.5194/acp-2016-136, 2016.

Hellenbrandt, M.: The Inorganic Crystal Structure Database (ICSD) - Present and Future, Crystallogr. Rev., 10, 17–22, doi:10.1080/08893110410001664882, 2004.

Hinds, W.: Aerosol Technology Properties, Behavior, and Measurement of Airborne Particles 2nd Edition, John Wiley & Sons, Inc., 1999.

Hiranuma, N., Hoffmann, N., Kiselev, A., Dreyer, A., Zhang, K., Kulkarni, G., Koop, T., and Möhler, O.: Influence of surface morphology on the immersion mode ice nucleation efficiency of hematite particles, Atmos. Chem. Phys., 14, 2315–2324, doi:10.5194/acp-14-2315-2014, 2014.



Hiranuma, N., Augustin-Bauditz, S., Bingemer, H., Budke, C., Curtius, J., Danielczok, A., Diehl, K., Dreischmeier, K., Ebert, M., Frank, F., Hoffmann, N., Kandler, K., Kiselev, A., Koop, T., Leisner, T., Möhler, O., Nillius, B., Peckhaus, A., Rose, D., Weinbruch, S., Wex, H., Boose, Y., DeMott, P. J., Hader, J. D., Hill, T. C. J., Kanji, Z. A., Kulkarni, G., Levin, E. J. T., McCluskey, C. S., Murakami, M., Murray, B. J., Niedermeier, D., Petters, M. D., O'Sullivan, D., Saito, A., Schill, G. P., Tajiri, T., Tolbert, M. A., Welti, A., Whale, T. F., Wright, T. P., and Yamashita, K.: A comprehensive laboratory study on the immersion freezing behavior of illite NX particles: a comparison of 17 ice nucleation measurement techniques, Atmos. Chem. Phys., 15, 2489–2518, doi:10.5194/acp-15-2489-2015, 2015.

Hobbs, P. V. and Rangno, A. L.: Ice Particle Concentrations in Clouds, J. Atmos. Sci., 42, 2523–2549, doi:10.1175/1520-0469(1985)042<2523:IPCIC>2.0.CO;2, 1985.

Hoffer, T. E.: A laboratory investigation of droplet freezing, J. Meteor., 18, 766–778, doi:10.1175/1520-0469(1961)018<0766:ALIODF>2.0.CO;2, 1961.

Hoose, C. and Möhler, O.: Heterogeneous ice nucleation on atmospheric aerosols: a review of results from laboratory experiments, Atmos. Chem. Phys., 12, 9817–9854, doi:10.5194/acp-12-9817-2012, 2012.

Ignatius, K., Kristensen, T. B., Järvinen, E., Nichman, L., Fuchs, C., Gordon, H., Herenz, P., Hoyle, C. R., Duplissy, J., Garimella, S., Dias, A., Frege, C., Höppel, N., Tröstl, J., Wagner, R., Yan, C., Amorim, A., Baltensperger, U., Curtius, J., Donahue, N. M., Gallagher, M. W., Kirkby, J., Kulmala, M., Möhler, O., Saathoff, H., Schnaiter, M., Tomé, A., Virtanen, A., Worsnop, D., and Stratmann, F.: Heterogeneous ice nucleation of viscous secondary organic aerosol produced from ozonolysis of $\alpha$-pinene, Atmos. Chem. Phys. Discuss., 15, 35 719–35 752, doi:10.5194/acpd-15-35719-2015, 2015.

Isono, K.: On ice-crystal nuclei and other substances found in snow crystals, J. Meteor., 12, 456–462, doi:10.1175/1520-0469(1955)012<0456:OICNAO>2.0.CO;2, 1955.

Kandler, K., Benker, N., Bundke, U., Cuevas, E., Ebert, M., Knippertz, P., Rodríguez, S., Schütz, L., and Weinbruch, S.: Chemical composition and complex refractive index of Saharan Mineral Dust at Izaña, Tenerife (Spain) derived by electron microscopy, Atmos. Environ., 41, 8058–8074, doi:10.1016/j.atmosenv.2007.06.047, 2007.

Kandler, K., Schütz, L., Deutscher, C., Ebert, M., Hofmann, H., Jäckl, S., Jaenicke, R., Knippertz, P., Lieke, K., Massling, A., and et al.: Size distribution, mass concentration, chemical and mineralogical composition and derived optical parameters of the boundary layer aerosol at Tinfou, Morocco, during SAMUM 2006, Tellus B, 61, 32–50, doi:10.1111/j.1600-0889.2008.00385.x, 2009.

Kanji, Z., Welti, A., Chou, C., Stetzer, O., and Lohmann, U.: Laboratory studies of immersion and deposition mode ice nucleation of ozone aged mineral dust particles, Atmos. Chem. Phys., 13, 9097 – 9118, doi:10.5194/acp-13-9097-2013, 2013.

Kaufmann, L., Marcolli, C., Hofer, J., Pinti, V., Hoyle, C. R., and Peter, T.: Ice nucleation efficiency of natural dust samples in the immersion mode, Atmos. Chem. Phys. Discuss., 2016, 1–46, doi:10.5194/acp-2016-337, 2016.

Knippertz, P. and Stuut, J.-B. W., eds.: Mineral Dust: A Key Player in the Earth System, Springer Dordrecht Heidelberg New York London, doi:10.1007/978-94-017-8978-3, 2014.

Knopf, D. A., Alpert, P. A., Wang, B., and Aller, J. Y.: Stimulation of ice nucleation by marine diatoms, Nature Geosci, 4, 88–90, doi:10.1038/ngeo1037, 2011.

Knopf, D. A., Alpert, P. A., Wang, B., O'Brien, R. E., Kelly, S. T., Laskin, A., Gilles, M. K., and Moffet, R. C.: Microspectroscopic imaging and characterization of individually identified ice nucleating particles from a case field study, J. Geophys. Res. Atmos., 119, 10,365–10,381, doi:10.1002/2014JD021866, 2014.

Krog, J. O., Zachariassen, K. E., Larsen, B., and Smidsrod, O.: Thermal buffering in Afro-alpine plants due to nucleating agent-induced water freezing, Nature, 282, 300–301, doi:10.1038/282300a0, 1979.



Kulkarni, G., China, S., Liu, S., Nandasiri, M., Sharma, N., Wilson, J., Aiken, A. C., Chand, D., Laskin, A., Mazzoleni, C., Pekour, M., Shilling, J., Shutthanandan, V., Zelenyuk, A., and Zaveri, R. A.: Ice nucleation activity of diesel soot particles at cirrus relevant temperature conditions: Effects of hydration, secondary organics coating, soot morphology, and coagulation, Geophys. Res. Lett., 43, 3580–3588, doi:10.1002/2016GL068707, 2016.

Kumai, M.: Identification of Nuclei and Concentrations of Chemical Species in Snow Crystals Sampled at the South Pole, J. Atmos. Sci., 33, 833–841, doi:10.1175/1520-0469(1976)033<0833:IONACO>2.0.CO;2, 1976.

Leinen, M., Prospero, J. M., Arnold, E., and Blank, M.: Mineralogy of aeolian dust reaching the North Pacific Ocean: 1. Sampling and analysis, J. Geophys. Res. Atmos., 99, 21 017–21 023, doi:10.1029/94JD01735, 1994.

Lohmann, U. and Feichter, J.: Global indirect aerosol effects: a review, Atmos. Chem. Phys., 5, 715–737, 2005.

Lüönd, F., Stetzer, O., Welti, A., and Lohmann, U.: Experimental study on the ice nucleation ability of size-selected kaolinite particles in the immersion mode, J. Geophys. Res. Atmos., 115, 1–14, doi:10.1029/2009JD012959, 2010.

Marcolli, C.: Deposition nucleation viewed as homogeneous or immersion freezing in pores and cavities, Atmos. Chem. Phys., 14, 2071–2104, doi:10.5194/acp-14-2071-2014, 2014.

Mason, B. J. and Ludlam, F. H.: The microphysics of clouds, Rep. Prog. Phys., 14, 147–195, 1950.

Meola, M., Lazzaro, A., and Zeyer, J.: Bacterial composition and survival on Sahara dust particles transported to the European Alps, Front. Microbiol., 6, doi:10.3389/fmicb.2015.01454, 2015.

Möhler, O., Field, P., Connolly, P., Benz, S., Saathoff, H., Schnaiter, M., Wagner, R., Cotton, R., Krämer, M., Mangold, A., and Heymsfield, A.: Efficiency of the deposition mode ice nucleation on mineral dust particles, Atmos. Chem. Phys., 6, 3007–3021, 2006.

Möhler, O., Georgakopoulos, D. G., Morris, C. E., Benz, S., Ebert, V., Hunsmann, S., Saathoff, H., Schnaiter, M., and Wagner, R.: Heterogeneous ice nucleation activity of bacteria: new laboratory experiments at simulated cloud conditions, Biogeosciences, 5, 1425–1435, doi:10.5194/bg-5-1425-2008, 2008.

Murray, B. J., Wilson, T. W., Dobbie, S., Cui, Z., Al-Jumur, S. M. R. K., Möhler, O., Schnaiter, M., Wagner, R., Benz, S., Niemand, M., Saathoff, H., Ebert, V., Wagner, S., and Karcher, B.: Heterogeneous nucleation of ice particles on glassy aerosols under cirrus conditions, Nature Geosci, 3, 233–237, doi:10.1038/ngeo817, 2010.

Murray, B. J., Broadley, S. L., Wilson, T. W., Atkinson, J. D., and Wills, R. H.: Heterogeneous freezing of water droplets containing kaolinite particles, Atmos. Chem. Phys., 11, 4191 – 4207, doi:10.5194/acp-11-4191-2011, 2011.

Murray, B. J., O'Sullivan, D., Atkinson, J. D., and Webb, M. E.: Ice nucleation by particles immersed in supercooled cloud droplets, Chem. Soc. Rev., 41, 6519, doi:10.1039/c2cs35200a, 2012.

Nicolet, M., Stetzer, O., Lüönd, F., Möhler, O., and Lohmann, U.: Single ice crystal measurements during nucleation experiments with the depolarization detector IODE, Atmos. Chem. Phys., 10, 313–325, 2010.

Niedermeier, D., Shaw, R. A., Hartmann, S., Wex, H., Clauss, T., Voigtländer, J., and Stratmann, F.: Heterogeneous ice nucleation: exploring the transition from stochastic to singular freezing behavior, Atmos. Chem. Phys., 11, 8767–8775, doi:10.5194/acp-11-8767-2011, 2011.

Niemand, M., Möhler, O., Vogel, B., Vogel, H., Hoose, C., Connolly, P., Klein, H., Bingemer, H., DeMott, P., Skrotzki, J., and Leisner, T.: A particle-surface-area-based parameterization of immersion freezing on desert dust particles, J. Atmos. Sci., 69, 3077–3092, 2012.

Peckhaus, A., Kiselev, A., Hiron, T., Ebert, M., and Leisner, T.: A comparative study of K-rich and Na/Ca-rich feldspar ice nucleating particles in a nanoliter droplet freezing assay, Atmos. Chem. Phys. Discuss., 2016, 1–43, doi:10.5194/acp-2016-72, 2016.

Perlwitz, J. P., Pérez García-Pando, C., and Miller, R. L.: Predicting the mineral composition of dust aerosols - Part 1: Representing key processes, Atmos. Chem. Phys., 15, 11 593–11 627, doi:10.5194/acp-15-11593-2015, 2015.



Pinti, V., Marcolli, C., Zobrist, B., Hoyle, C. R., and Peter, T.: Ice nucleation efficiency of clay minerals in the immersion mode, Atmos. Chem. Phys., 12, 5859–5878, doi:10.5194/acp-12-5859-2012, 2012.

Prenni, A. J., Petters, M. D., Faulhaber, A., Carrico, C. M., Ziemann, P. J., Kreidenweis, S. M., and DeMott, P. J.: Heterogeneous ice nucleation measurements of secondary organic aerosol generated from ozonolysis of alkenes, Geophys. Res. Lett., 36, L06 808, doi:10.1029/2008GL036957, l06808, 2009.

Rietveld, H. M.: A profile refinement method for nuclear and magnetic structures, J. Appl. Crystallogr., 2, 65–71, doi:10.1107/S0021889869006558, 1969.

Roberts, P. and Hallett, J.: A laboratory study of the ice nucleating properties of some mineral particulates, Quart. J. Roy. Meteor. Soc., 95, 204–205, doi:10.1002/qj.49709540317, 1969.

Rogers, D. C.: Development of a continuous flow thermal gradient diffusion chamber for ice nucleation studies, Atmos. Res., 22, 149–181, 1988.

Schaefer, V. J.: The Production of Ice Crystals in a Cloud of Supercooled Water Droplets, Science, 104, 457–459, doi:10.1126/science.104.2707.457, 1946.

Schnell, R. C. and Vali, G.: Biogenic Ice Nuclei: Part I. Terrestrial and Marine Sources, J. Atmos. Sci., 33, 1554–1564, doi:10.1175/1520-0469(1976)033<1554:BINPIT>2.0.CO;2, 1976.

Schütz, L. and Sebert, M.: Mineral aerosols and source identification, J. Aerosol Sci., 18, 1–10, doi:10.1016/0021-8502(87)90002-4, 1987.

Steinke, I.: Ice nucleation properties of mineral dusts, Ph.D. thesis, The Faculty of Physics and Astronomy – Institute of Environmental Physics, Heidelberg University, Heidelberg, 2013.

Stetzer, O., Baschek, B., Lüönd, F., and Lohmann, U.: The Zurich Ice Nucleation Chamber (ZINC)-A new instrument to investigate atmospheric ice formation, Aerosol Sci. Technol., 42, 64–74, doi:10.1080/02786820701787944, 2008.

Tobo, Y., Prenni, A. J., DeMott, P. J., Huffmann, A., McCluskey, C. S., Tian, G., Pöhlker, C., Pöschl, U., and Kreidenweis, S. M.: Biological aerosol particles as a key determinant of ice nuclei populations in a forest ecosystem, J. Geophys. Res. Atmos., 118, 1–11, doi:10.1002/jgrd.50801, 2013.

Vali, G.: Quantitative Evaluation of Experimental Results an the Heterogeneous Freezing Nucleation of Supercooled Liquids, J. Atmos. Sci., 28, 402–409, doi:10.1175/1520-0469(1971)028<0402:QEOERA>2.0.CO;2, 1971.

Vali, G., DeMott, P. J., Möhler, O., and Whale, T. F.: Technical Note: A proposal for ice nucleation terminology, Atmos. Chem. Phys., 15, 10 263–10 270, doi:10.5194/acp-15-10263-2015, 2015.

Welti, A., Lüönd, F., Stetzer, O., and Lohmann, U.: Influence of particle size on the ice nucleating ability of mineral dusts, Atmos. Chem. Phys., 9, 6705–6715, doi:10.5194/acp-9-6705-2009, 2009.

Welti, A., Lüönd, F., Kanji, Z., Stetzer, O., and Lohmann, U.: Time dependence of immersion freezing: an experimental study on size selected kaolinite particles, Atmos. Chem. Phys., 12, 9893–9907, 2012.

Welti, A., Kanji, Z. A., Lüönd, F., Stetzer, O., and Lohmann, U.: Exploring the Mechanisms of Ice Nucleation on Kaolinite: From Deposition Nucleation to Condensation Freezing, J. Atmos. Sci., 71, 16–36, doi:10.1175/JAS-D-12-0252.1, 2014.

Wilson, T. W., Ladino, L. A., Alpert, P. A., Breckels, M. N., Brooks, I. M., Browse, J., Burrows, S. M., Carslaw, K. S., Huffman, J. A., Judd, C., Kilthau, W. P., Mason, R. H., McFiggans, G., Miller, L. A., Najera, J. J., Polishchuk, E., Rae, S., Schiller, C. L., Si, M., Temprado, J. V., Whale, T. F., Wong, J. P. S., Wurl, O., Yakobi-Hancock, J. D., Abbatt, J. P. D., Aller, J. Y., Bertram, A. K., Knopf, D. A., and Murray, B. J.: A marine biogenic source of atmospheric ice-nucleating particles, Nature, 525, 234–238, doi:10.1038/nature14986, 2015.

Atmos. Chem. Phys. Discuss., doi:10.5194/acp-2016-438, 2016
Manuscript under review for journal Atmos. Chem. Phys.
Published: 2 June 2016


Atmospheric Chemistry and Physics Discussions

Zimmermann, F., Weinbruch, S., Schütz, L., Hofmann, H., Ebert, M., Kandler, K., and Worringen, A.: Ice nucleation properties of the most abundant mineral dust phases, J. Geophys. Res. Atmos., 113, 1–11, doi:10.1029/2008JD010655, 2008.

Zolles, T., Burkart, J., Häusler, T., Pummer, B., Hitzenberger, R., and Grothe, H.: Identification of Ice Nucleation Active Sites on Feldspar Dust Particles, J. Phys. Chem. A, 119, 2692–2700, doi:10.1021/jp509839x, 2015.

Atmos. Chem. Phys. Discuss., doi:10.5194/acp-2016-438, 2016
Manuscript under review for journal Atmos. Chem. Phys.
Published: 2 June 2016


Atmospheric Chemistry and Physics Discussions

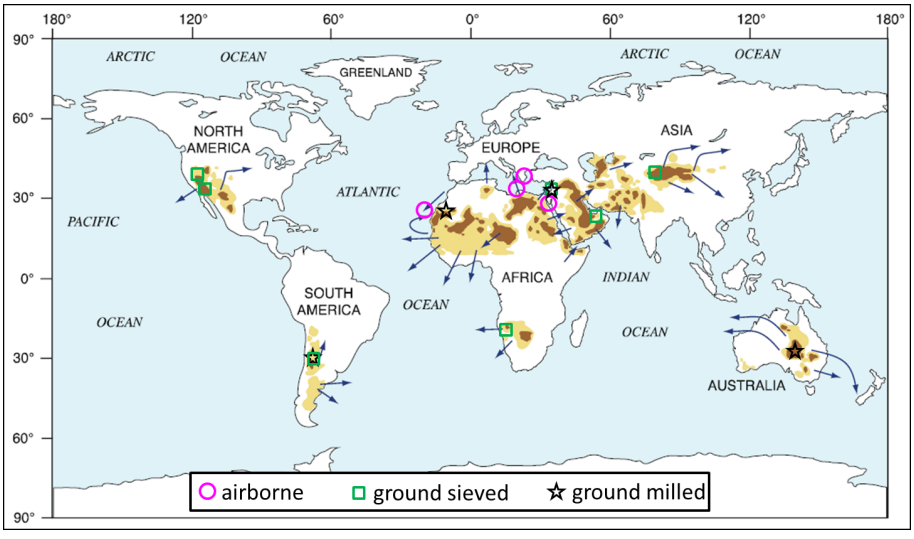


**Figure 1.** Collection sites of the dust samples. Green squares/black stars indicate sieved/milled samples which were collected directly from the surface, pink circles indicate samples that were collected either directly from the air or after deposition, resulting from transport to the location from the Sahara. See text for details on the collection methods and treatment after collection. The map was adapted from Knippertz and Stuut (2014) and is based on data from Total Ozone Mapping Spectrometer (TOMS) satellite data of the absorbing aerosol index ($AAI$). Dark brown color indicates 21 - 31 days of $AAI > 0.7$, i.e. significant amounts of dust or smoke. Yellow indicates 7 - 21 days of $AAI > 0.7$. Arrows show typical dust transport pathways in the atmosphere.

Atmos. Chem. Phys. Discuss., doi:10.5194/acp-2016-438, 2016
Manuscript under review for journal Atmos. Chem. Phys.
Published: 2 June 2016


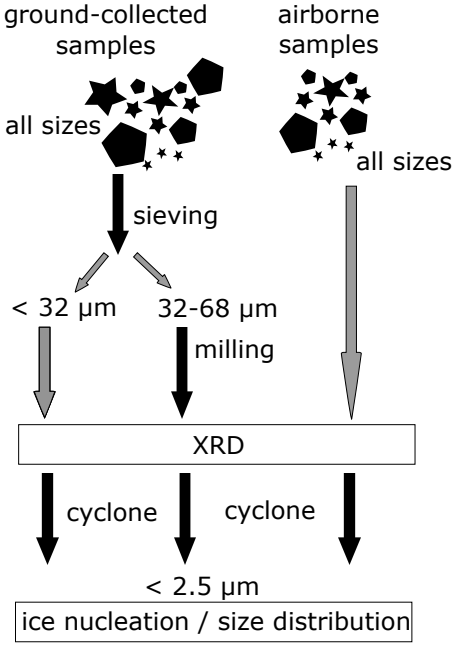


**Figure 2.** Schematic of size fractions used for XRD and ice nucleation.

Atmos. Chem. Phys. Discuss., doi:10.5194/acp-2016-438, 2016
Manuscript under review for journal Atmos. Chem. Phys.
Published: 2 June 2016


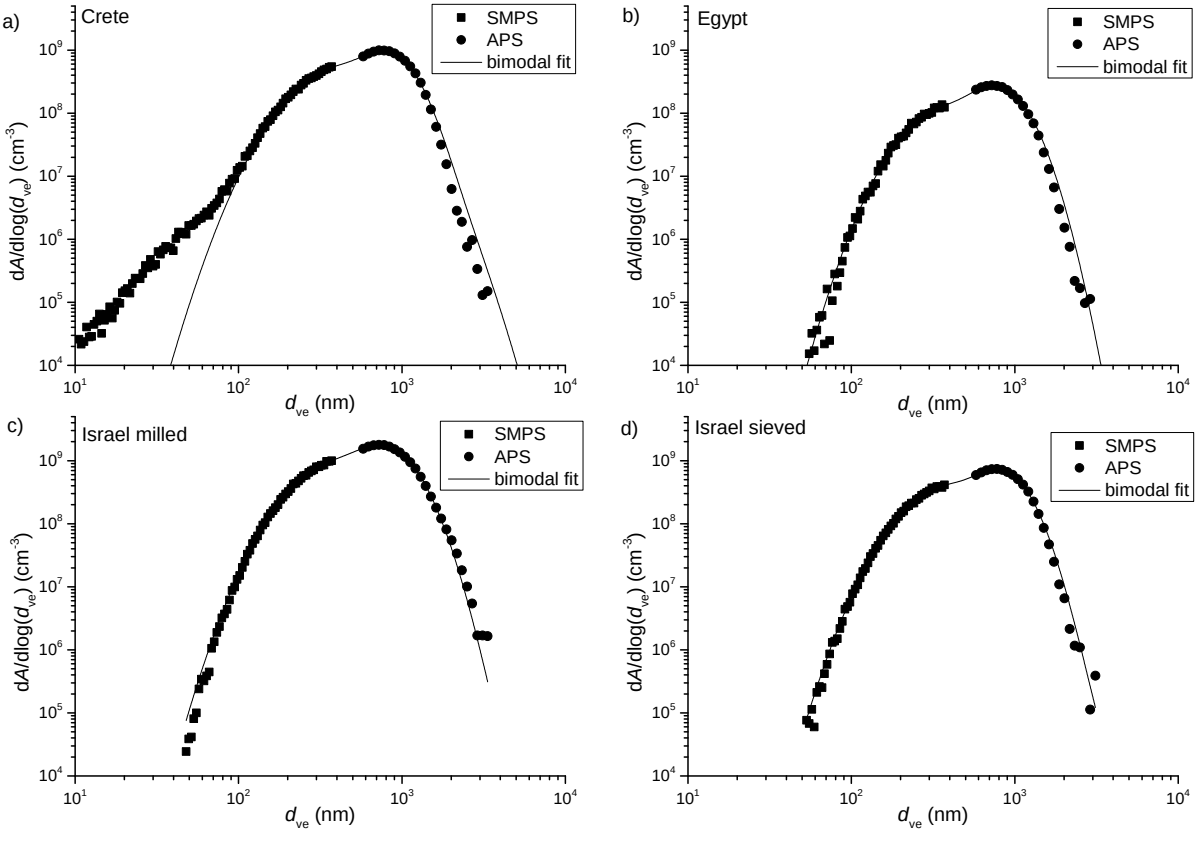


**Figure 3.** Sample surface area distribution of four of the dust samples with bimodal fits.

Atmos. Chem. Phys. Discuss., doi:10.5194/acp-2016-438, 2016
Manuscript under review for journal Atmos. Chem. Phys.
Published: 2 June 2016


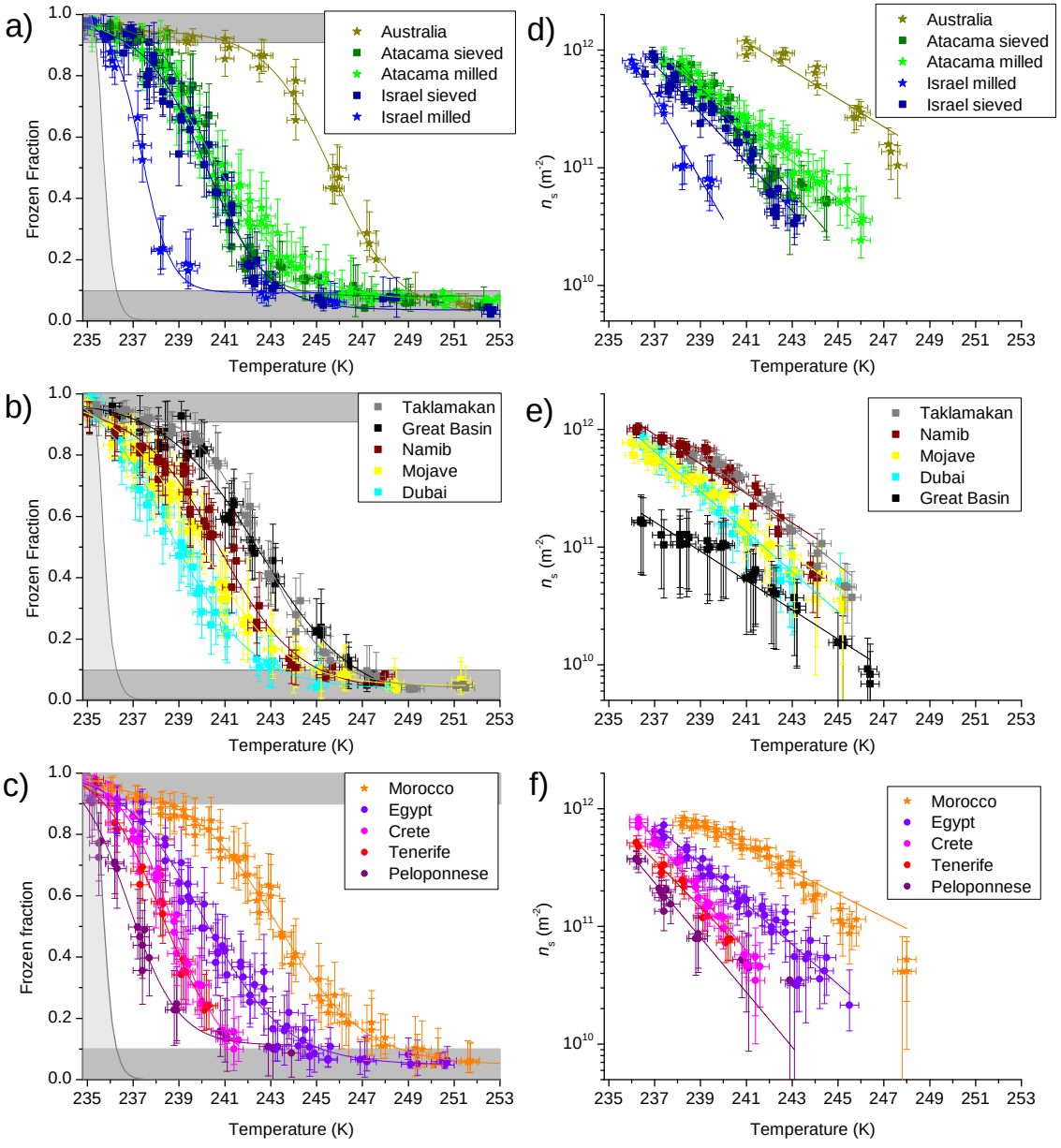


**Figure 4.** Frozen fraction of non-Saharan samples (panel a and b) and c) samples originating in the Sahara. Lines are best sigmoidal fits. Squares: surface-collected and sieved, stars: surface-collected and milled and circles: airborne samples. The light gray area is the homogeneous freezing regime and the two dark gray rectangles show the upper and lower detection limits of IODE. Ice-active surface site density of non-Saharan (panel d and e) and f) Saharan samples. Lines are best exponential fits. The fit parameters are given in Table 4.

Atmos. Chem. Phys. Discuss., doi:10.5194/acp-2016-438, 2016
Manuscript under review for journal Atmos. Chem. Phys.
Published: 2 June 2016


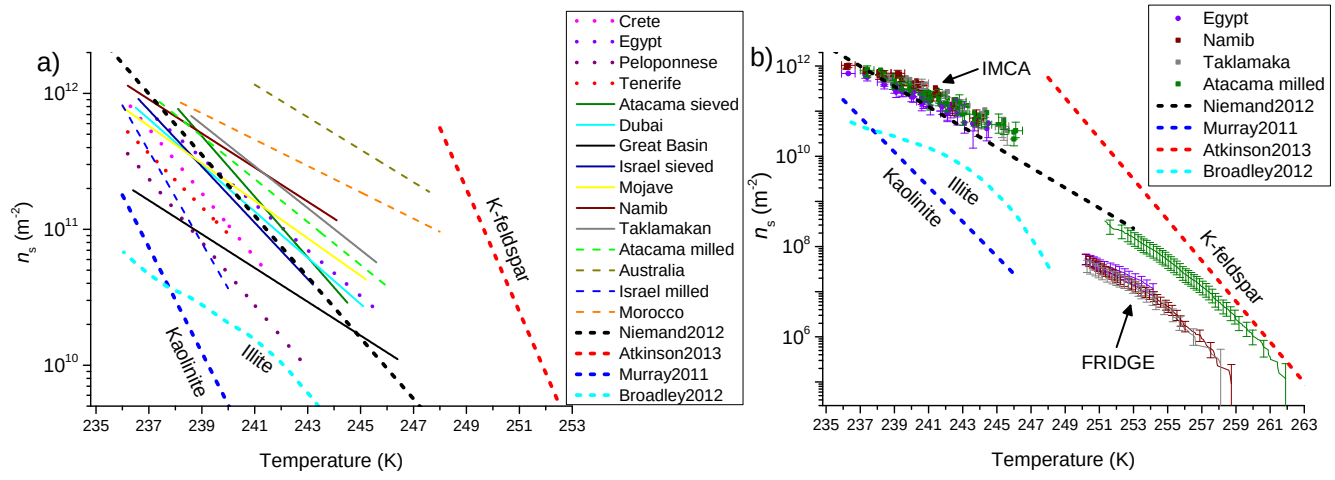


**Figure 5.** a) Ice-active surface site density fits of all dust samples. The fit parameters are given in Table 4. Solid lines indicate surface-collected and sieved samples, dashed lines surface-collected and milled samples and dotted lines airborne samples. b) Full temperature range measurements by IMCA and FRIDGE. Colors and markers are the same as in Fig. 4. The FRIDGE data points are single measurement points but for visual clarity are shown as lines. Error bars are drawn for every 10$^{th}$ data point. Parameterizations for desert dust (Niemand et al., 2012), kaolinite (Murray et al., 2011) and K-feldspar (Atkinson et al., 2013) are given as thick dashed lines.

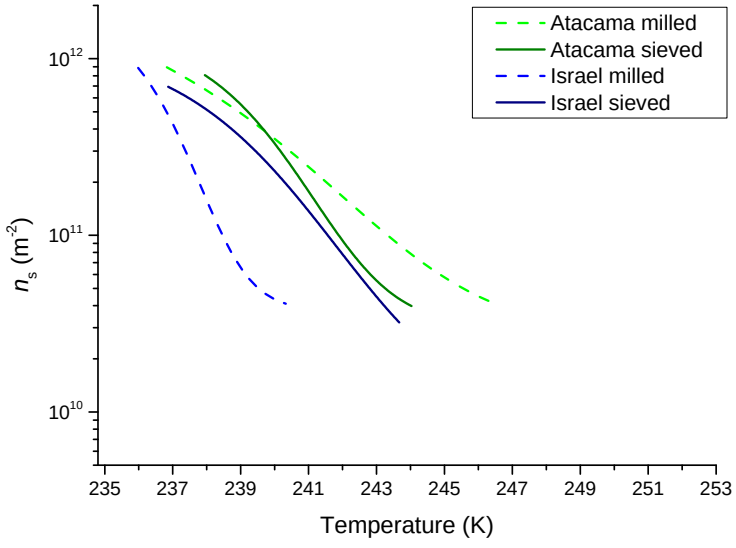


**Figure 6.** Comparison of ice-active surface site density of milled and sieved samples.

Atmos. Chem. Phys. Discuss., doi:10.5194/acp-2016-438, 2016
Manuscript under review for journal Atmos. Chem. Phys.
Published: 2 June 2016


Atmospheric Chemistry and Physics Discussions

**Table 1.** Overview of the dust size distribution parameters: the weighted mean surface area per particle $\overline{A_{\mathrm{ve,w}}}$ with relative error $\delta(\overline{A_{\mathrm{ve,w}}})$ and the corresponding diameter of a particle with this surface area: $\overline{d_{\mathrm{ve,w}}}$ with the relative error $\delta(\overline{d_{\mathrm{ve,w}}})$.

| Collection site | type | $\overline{A_{\mathrm{ve,w}}}$ ($\mu$m$^2$) | $\delta(\overline{A_{\mathrm{ve,w}}})$ | $\overline{d_{\mathrm{ve,w}}}$ (nm) | $\delta(\overline{d_{\mathrm{ve,w}}})$ |
|---|---|---|---|---|---|
| Atacama | sieved | 2.79 | 0.17 | 940 | 0.08 |
| Atacama | milled | 2.56 | 0.24 | 897 | 0.11 |
| Australia | milled | 2.14 | 0.09 | 824 | 0.05 |
| Crete | airborne | 3.04 | 0.08 | 983 | 0.04 |
| Dubai | sieved | 2.18 | 0.18 | 830 | 0.09 |
| Egypt | airborne | 3.26 | 0.12 | 1017 | 0.06 |
| Great Basin | sieved | 16.4 | 0.64 | 2133 | 0.39 |
| Peloponnese | airborne | 3.27 | 0.06 | 1020 | 0.03 |
| Israel | sieved | 3.32 | 0.14 | 1024 | 0.07 |
| Israel | milled | 2.57 | 0.12 | 904 | 0.06 |
| Mojave | sieved | 2.99 | 0.14 | 973 | 0.07 |
| Morocco | milled | 2.81 | 0.13 | 960 | 0.07 |
| Namib | sieved | 2.08 | 0.07 | 813 | 0.03 |
| Taklamakan | sieved | 3.69 | 0.19 | 1079 | 0.09 |
| Tenerife | airborne | 3.55 | 0.12 | 1061 | 0.06 |

Atmos. Chem. Phys. Discuss., doi:10.5194/acp-2016-438, 2016
Manuscript under review for journal Atmos. Chem. Phys.
Published: 2 June 2016


Atmospheric Chemistry and Physics Discussions

**Table 2.** Mineralogical composition in wt% and uncertainty from the Rietveld refinement using AutoQuan. Where microcline and orthoclase are present in the same sample, their individual fraction could not be distinguished. The Namib sample was taken from Kaufmann et al. (2016) who did not provide a Rietveld fit uncertainty from AutoQuan but estimate 15 % accuracy.

| Mineral Type | Atacama milled | Atacama sieved | Australia milled | Cyprus airborne | Dubai sieved | Egypt airborne | Great Basin sieved | Namib sieved |
|---|---|---|---|---|---|---|---|---|
| Ankerite | | | | | | | | 23 |
| Biotite | 2.8±0.6 | | | | 1.0±0.5 | | | |
| Calcite | | | | 25.0±0.6 | 37.2±0.6 | 29.2±1.2 | 12.9±0.4 | 29 |
| Chlorite | | | | 3.8±0.6 | 14.0±1.2 | 8.2 ±1.3 | 2.1 ±0.3 | |
| Cristobalite | 14.0±1.7 | 12.7±1.9 | | | | | | |
| Dolomite | | | | 3.1±0.7 | 6.8 ±0.5 | 8.1 ±1.3 | 1.9±0.3 | 27 |
| Gypsum | | | | 3.7±0.7 | | 5.5±0.9 | 2.8±0.3 | |
| Halite | | | | 1.0±0.2 | | 4.4±0.5 | 2.1±0.1 | |
| Hematite | 3.2±0.4 | 4.0±0.5 | 0.6±0.1 | 0.9±0.2 | 1.4±0.2 | | 0.9±0.2 | |
| Hornblende | 1.8±0.6 | 1.3±0.7 | | 1.5±0.4 | 1.8±0.5 | | 1.0±0.5 | |
| Illite | | 10.0±1.0 | | | | | | |
| Kaolinite | | | | 12.4±1.0 | | 10.5±1.5 | 17.7±0.9 | |
| Microcline | | | 3.9±0.5 | | | | 30.1±0.8 | |
| Muscovite | 2.4±0.6 | 4.2±1.0 | | | 4.1±0.5 | 7.6±1.3 | 4.0±0.5 | 10 |
| Orthoclase | 22.3±0.9 | 11.8±0.9 | 4.2±0.5 | 5.1±0.6 | 2.4±0.4 | 3.5±1.1 | | |
| Palygorskite | | | | 4.5±0.5 | 3.4±0.5 | | | |
| Na-Plagioclase | 43.2±1.4 | 39.3±1.6 | | 7.2±0.4 | 9.5±0.4 | | 3.7±0.3 | |
| Smectite | | | | | | | | 1 |
| Quartz | 10.4±0.4 | 16.7±0.6 | 91.3±0.5 | 23.0±0.5 | 13.3±0.3 | 23.0±1.1 | 20.1±0.5 | 1 |
| others | | | | | 5.1±0.4 | | 0.7±0.3 | 7 |

Atmos. Chem. Phys. Discuss., doi:10.5194/acp-2016-438, 2016
Manuscript under review for journal Atmos. Chem. Phys.
Published: 2 June 2016


Atmospheric Chemistry and Physics Discussions

**Table 3.** Mineralogical composition in wt% and uncertainty from the Rietveld refinement using AutoQuan continued. Where microcline and orthoclase are present in the same sample, their individual fraction could not be distinguished.

| Mineral Type | Peloponnese airborne | Israel sieved | Israel milled | Mojave sieved | Morocco milled | Taklamakan sieved | Tenerife airborne |
|---|---|---|---|---|---|---|---|
| Biotite | | | | | | | |
| Calcite | 33.0±0.6 | 67.2±1.2 | 81.0±1.0 | 13.0±0.5 | 6.0±0.3 | 14.6±0.4 | 8.1±0.5 |
| Chlorite | 2.7±9.5 | | | 8.5±1.4 | 5.9±1.0 | 7.1 ±0.9 | 3.3 ±0.6 |
| Cristobalite | | | | | | | |
| Dolomite/Ankerite | 4.6±0.5 | 8.0±0.4 | 1.3±0.2 | 10.6±0.7 | 1.4±0.6 | 4.6±0.5 | |
| Gypsum | | 1.2±0.2 | | | | 1.8±0.5 | 3.2±0.5 |
| Halite | | | | | | 0.9±0.2 | 0.6±0.1 |
| Hematite | 0.6±0.2 | 0.5±0.1 | | 1.0±0.3 | 2.7±0.5 | | 0.6±0.2 |
| Hornblende | 1.5±0.5 | | | 1.3±0.6 | | 5.4±0.5 | |
| Illite | 12.5±1.0 | 4.2±1.6 | 0.3±0.2 | 17.4±1.4 | 3.0±0.7 | | 14.2±1.1 |
| Kaolinite | 7.8±0.7 | 0.8±0.6 | 0.3±0.3 | | | | 24.3±1.5 |
| Microcline | | 1.7±0.4 | 1.3±0.4 | | 3.8±1.0 | | 6.0±0.7 |
| Muscovite | 4.8±0.8 | | 1.1±0.5 | 11.25±0.8 | 1.8±0.3 | 8.0±0.6 | 11.0±0.8 |
| Orthoclase | 4.0±0.5 | | | 5.7±0.5 | 2.2±0.6 | 5.3±0.6 | |
| Palygorskite | 5.3±0.8 | 2.2±0.4 | 1.6±0.4 | | | | 4.8±0.6 |
| Na-Plagioclase | 5.0±0.4 | 2.3±0.5 | 0.7±0.3 | 16.3±0.7 | 8.8±0.4 | 19.3±0.8 | 4.8±0.5 |
| Smectite | | 4.5±0.6 | 6.4±1.2 | | | | |
| Quartz | 17.9±0.4 | 7.3±0.3 | 6.1±0.2 | 14.7±0.5 | 63.8±1.2 | 33.1±0.7 | 15.7±0.6 |
| others | 0.5±0.1 | | | 0.2±0.1 | | | |

Atmos. Chem. Phys. Discuss., doi:10.5194/acp-2016-438, 2016
Manuscript under review for journal Atmos. Chem. Phys.
Published: 2 June 2016


Atmospheric Chemistry and Physics Discussions

**Table 4.** Overview of the dust $n_s$ fit parameters $a$ and $b$, the resulting $R^2$ and the number of data points in each fit, $N$.

| Collection site | type | $a$ ($K^{-1}$) | $b$ | $R^2$ | $N$ |
|---|---|---|---|---|---|
| Atacama | sieved | 0.513 | 9.39 | 0.91 | 36 |
| Atacama | milled | 0.363 | 14.50 | 0.96 | 50 |
| Australia | milled | 0.274 | 18.93 | 0.89 | 16 |
| Crete | airborne | 0.545 | 7.32 | 0.98 | 30 |
| Dubai | sieved | 0.391 | 13.04 | 0.96 | 35 |
| Egypt | airborne | 0.390 | 13.22 | 0.96 | 41 |
| Great Basin | sieved | 0.286 | 15.47 | 0.93 | 35 |
| Peloponnese | airborne | 0.535 | 6.84 | 0.95 | 17 |
| Israel | sieved | 0.477 | 10.11 | 0.91 | 39 |
| Israel | milled | 0.777 | -1.43 | 0.95 | 13 |
| Mojave | sieved | 0.317 | 15.62 | 0.96 | 46 |
| Morocco | milled | 0.223 | 19.67 | 0.94 | 45 |
| Namib | sieved | 0.289 | 17.09 | 0.93 | 33 |
| Taklamakan | sieved | 0.355 | 15.00 | 0.93 | 21 |
| Tenerife | airborne | 0.455 | 10.16 | 0.97 | 14 |

**Table 5.** Overview of the Pearson correlation coefficients of the sum of ice-active minerals and $n_s$ at different temperatures. The last three columns are only samples where the mineralogy is representative for the size fraction smaller than 2.5 $\mu$m. The Namib sample was only included in the correlation with calcite because it does not contain feldspars, illite and kaolinite and only traces of quartz.

| $n_s$ at | 253 K | 245 K | 243 K | 240 K | 238 K | 243 K | 240 K | 238 K |
|---|---|---|---|---|---|---|---|---|
| number of samples | 3 | 7 | 11 | 14 | 14 | 4 | 6 | 6 |
| K-feldspar | 0.99 | -0.24 | -0.07 | 0.20 | 0.23 | -0.22 | 0.91 | 0.79 |
| feldspars | 0.93 | -0.37 | -0.23 | 0.06 | 0.17 | 0.99 | 0.99 | 0.92 |
| quartz | -0.92 | 0.91 | 0.92 | 0.80 | 0.60 | 0.99 | -0.11 | 0.03 |
| illite | | -0.21 | -0.29 | -0.43 | -0.34 | -0.63 | -0.41 | -0.37 |
| kaolinite | -0.46 | -0.39 | -0.28 | -0.23 | -0.16 | -0.38 | -0.50 | -0.45 |
| feldspars + quartz | 0.75 | 0.78 | 0.70 | 0.74 | 0.64 | 0.75 | 0.97 | 0.93 |
| feldspars + quartz + illite | 0.75 | 0.77 | 0.66 | 0.68 | 0.60 | 0.74 | 0.92 | 0.89 |
| feldspars + quartz + kaolinite | 0.82 | 0.73 | 0.66 | 0.69 | 0.61 | 0.79 | 0.84 | 0.83 |
| feldspars + quartz + illite + kaolinite | 0.82 | 0.76 | 0.58 | 0.61 | 0.55 | 0.79 | 0.75 | 0.74 |
| calcite | -0.86 | -0.56 | -0.41 | -0.41 | -0.35 | -0.41 | -0.49 | -0.55 |